Charmless hadronic $B_c \to VA, AA$ decays in the perturbative QCD approach

Xin Liu* and Zhen-Jun Xiao†

Department of Physics and Institute of Theoretical Physics,
Nanjing Normal University, Nanjing,
Jiangsu 210046, People's Republic of China

(Dated: April 12, 2010)

Abstract

In this work, we calculate the branching ratios (BRs) and the polarization fractions of sixty two charmless two-body B_c meson decays into final states involving one vector and one axial-vector meson (VA) or two axial-vector mesons(AA) within the framework of perturbative QCD approach systematically, where A is either a ${}^3P_1$ or ${}^1P_1$ axial-vector meson. All considered decay channels can only occur through the annihilation topologies in the standard model. Based on the perturbative calculations and phenomenological analysis, we find the following results: (i) the CP-averaged BRs of the considered sixty two B_c decays are in the range of 10^{-5} to 10^{-9}; (ii) since the behavior for ${}^1P_1$ meson is much different from that of ${}^3P_1$ meson, the BRs of $B_c \to A({}^1P_1)(V, A({}^1P_1))$ decays are generally larger than that of $B_c \to A({}^3P_1)(V, A({}^3P_1))$ decays in the perturbative QCD approach; (iii) many considered decays modes, such as $B_c \to a_1(1260)^+\omega$, $b_1(1235)\rho$, etc, have sizable BRs within the reach of the LHCb experiments; (iv) the longitudinal polarization fractions of most considered decays are large and play the dominant role; (v) the perturbative QCD predictions for several decays involving mixtures of ${}^3P_1$ and/or ${}^1P_1$ mesons are highly sensitive to the values of the mixing angles, which will be tested by the ongoing LHC and forthcoming Super-B experiments; (vi) the CP-violating asymmetries of these considered B_c decays are absent in the standard model because only one type tree operator is involved.

PACS numbers: 13.25.Hw, 12.38.Bx, 14.40.Nd

* liuxin.physics@gmail.com
† xiaozhenjun@njnu.edu.cn

I. INTRODUCTION

Unlike the B_q meson with $q = (u, d, s)$, the B_c meson is the only heavy meson embracing two heavy quarks b and c simultaneously. Researchers believe that the B_c physics must be very rich if the statistics reaches high level. With the running of Large Hadron Collider(LHC) experiments, a great number of B_c meson events, about 10% of the total B meson data, will be collected and this will provide a new platform for both theorists and experimentalists to study the perturbative and nonperturbative QCD dynamics, final state interactions, even the new physics scenarios beyond the standard model(SM) [1].

Very recently, we studied the two-body charmless hadronic decays $B_c \to PP, PV/VP, VV$ and $B_c \to AP$ (here P, V and A stand for the light pseudo-scalar, vector and axial-vector mesons respectively) [2, 3]. All these decays can only occur via the annihilation type diagrams in the SM. Although the contributions induced by annihilation diagrams are suppressed in the decays of ordinary light B_q ($q = u, d, s$) mesons, they could be large and detected at LHC experiments [4] in B_c meson decays. According to the discussions as given in Ref. [4], the charmless hadronic B_c decays with decay rates at the level of 10^{-6} could be measured at the LHC experiments with the accuracy required for the phenomenological analysis, it is therefore believed that they can help the people to understand the annihilation decay mechanism in B physics well. In this paper, we will extend our previous studies of two-body B_c decays to $B_c \to VA$ and AA modes, which are also pure annihilation type decays, and expected to have rich physics since there are three polarization states involved in these decays.

In this paper, we will calculate the CP-averaged branching ratios (BRs) and polarization fractions of the sixty two charmless hadronic $B_c \to VA, AA$ decays by employing the low energy effective Hamiltonian [5] and the perturbative QCD (pQCD) factorization approach [6–8]. In the pQCD approach, the annihilation type diagrams can be calculated analytically, as have been done for example in Refs. [6, 7, 9–14]. First of all, the size of annihilation contributions is an important issue in the B meson physics, and has been studied extensively, for example, in Refs. [6, 7, 9, 10, 15, 16]. Second, the internal structure of the axial-vector mesons has been one of the hot topics in recent years [17–19]. Although many efforts on both theoretical and experimental sides have been made [20–26] to explore it through the studies for the relevant decay rates, CP-violating asymmetries, polarization fractions and form factors, etc., we currently still know little about the nature of the axial-vector mesons. Furthermore, through the polarization studies in the considered $B_c \to VA, AA$ decays, these channels can shed light on the underlying helicity structure of the decay mechanism.

The paper is organized as follows. In Sec. II, we present the formalism and give the essential input quantities, including the operator basis and the mixing angles between $^3P_1$ and/or $^1P_1$ mesons. The wave functions and distribution amplitudes for B_c and light vector and axial-vector mesons are also given here. Then we perform the perturbative calculations for considered decay channels in Sec. III. The analytic expressions of the decay amplitudes for all considered sixty two $B_c \to VA, AA$ decay modes are also collected in this section. The numerical results and phenomenological analysis are given in Sec. IV. The main conclusions and a short summary are presented in the last section.

II. INPUT QUANTITIES AND FORMALISM

In the following we shall briefly discuss the mixing of axial-vector mesons and summarize all the input quantities relevant to the present work, such as the operator basis, mixing angles,

wave functions and light-cone distribution amplitudes for light vector and axial-vector mesons. Finally, the formalism of pQCD approach will also be presented briefly.

A. Effective Hamiltonian

For those considered charmless hadronic B_c decays, the related weak effective Hamiltonian $H_{\rm eff}$ is given by [5]

$$H_{\rm eff} = \frac{G_F}{\sqrt{2}} \left[V^*_{cb} V_{uD} \left(C_1(\mu) O_1(\mu) + C_2(\mu) O_2(\mu) \right) \right] , \tag{1}$$

with the local four-quark tree operators $O_{1,2}$

$$\begin{aligned} O_1 &= \bar{u}_\beta \gamma^\mu (1-\gamma_5) D_\alpha \bar{c}_\beta \gamma^\mu (1-\gamma_5) b_\alpha , \\ O_2 &= \bar{u}_\beta \gamma^\mu (1-\gamma_5) D_\beta \bar{c}_\alpha \gamma^\mu (1-\gamma_5) b_\alpha , \end{aligned} \tag{2}$$

where V_{cb}, V_{uD} are the Cabibbo-Kobayashi-Maskawa (CKM) matrix elements, "D" denotes the light down quark d or s and $C_i(\mu)(i = 1, 2)$ are Wilson coefficients at the renormalization scale μ. For the Wilson coefficients $C_i(\mu)$, we will also use the leading order expressions, although the next-to-leading order calculations already exist in the literature [5]. This is the consistent way to cancel the explicit μ dependence in the theoretical formulas. For the renormalization group evolution of the Wilson coefficients from higher scale to lower scale, we use the formulas as given in Ref. [7] directly.

B. Mixtures and Mixing Angles

In the quark model, there exist two distinct types of light parity-even axial-vector mesons, namely, $^3P_1$ ($J^{\rm PC} = 1^{++}$) and $^1P_1 (J^{\rm PC} = 1^{+-})$. The $^3P_1$ nonet consists of $a_1(1260)$, $f_1(1285)$, $f_1(1420)$ and K_{1A} states, while the $^1P_1$ nonet has $b_1(1235)$, $h_1(1170)$, $h_1(1380)$ and K_{1B} states. In the SU(3) flavor limit, these mesons can not mix with each other. Because the s quark is heavier than u, d quarks, the physical mass eigenstates $K_1(1270)$ and $K_1(1400)$ are not purely 1^3P_1 or 1^1P_1 states, but believed to be mixtures of K_{1A} and K_{1B}[1]. Analogous to η and η' system, the flavor-singlet and flavor-octet axial-vector meson can also mix with each other. It is worth mentioning that the mixing angles can be determined by the relevant data, but unfortunately, there is no enough data now for these mesons which leaves the mixing angles basically free parameters.

The physical states $K_1(1270)$ and $K_1(1400)$ can be written as the mixtures of the K_{1A} and K_{1B} states:

$$\begin{pmatrix} K_1(1270) \\ K_1(1400) \end{pmatrix} = \begin{pmatrix} \sin\theta_K & \cos\theta_K \\ \cos\theta_K & -\sin\theta_K \end{pmatrix} \begin{pmatrix} K_{1A} \\ K_{1B} \end{pmatrix} \tag{3}$$

The mixing angle θ_K still not be well determined because of the poor experimental data. In this paper, for simplicity, we will adopt two reference values as those used in Ref. [19]: $\theta_K = \pm 45^\circ$.

[1] For the sake of simplicity, we will adopt the forms a_1, b_1, K', K'', f', f'', h' and h'' to denote the axial-vector mesons $a_1(1260)$, $b_1(1235)$, $K_1(1270)$, $K_1(1400)$, $f_1(1285)$, $f_1(1420)$, $h_1(1170)$ and $h_1(1380)$ correspondingly in the following sections, unless otherwise stated. We will also use K_1, f_1 and h_1 to denote $K_1(1270)$ and $K_1(1400)$, $f_1(1285)$ and $f_1(1420)$, and $h_1(1170)$ and $h_1(1380)$ for convenience unless explicitly otherwise stated.

Analogous to the η-η' mixing in the pseudoscalar sector, the $h_1(1170)$ and $h_1(1380)$ (1^1P_1 states) system can be mixed in terms of the pure singlet $|h_1\rangle$ and octet $|h_8\rangle$,

$$\begin{pmatrix} h_1(1170) \\ h_1(1380) \end{pmatrix} = \begin{pmatrix} \cos\theta_1 & \sin\theta_1 \\ -\sin\theta_1 & \cos\theta_1 \end{pmatrix} \begin{pmatrix} h_1 \\ h_8 \end{pmatrix} \tag{4}$$

Likewise, $f_1(1285)$ and $f_1(1420)$ (the 1^3P_1 states) will mix in the form of

$$\begin{pmatrix} f_1(1285) \\ f_1(1420) \end{pmatrix} = \begin{pmatrix} \cos\theta_3 & \sin\theta_3 \\ -\sin\theta_3 & \cos\theta_3 \end{pmatrix} \begin{pmatrix} f_1 \\ f_8 \end{pmatrix} \tag{5}$$

where the component of h_1, f_1 and h_8, f_8 can be written as

$$\begin{aligned} |h_1\rangle = |f_1\rangle &= \frac{1}{\sqrt{3}}\left(|\bar{q}q\rangle + |\bar{s}s\rangle\right), \\ |h_8\rangle = |f_8\rangle &= \frac{1}{\sqrt{6}}\left(|\bar{q}q\rangle - 2|\bar{s}s\rangle\right), \end{aligned} \tag{6}$$

where $q = (u, d)$. The values of the mixing angles for 1^1P_1 and 1^3P_1 states are chosen as [19]:

$$\theta_1 = 10^\circ \quad or \quad 45^\circ; \qquad \theta_3 = 38^\circ \quad or \quad 50^\circ. \tag{7}$$

C. Wave Functions and Distribution Amplitudes

In order to calculate the decay amplitude, we should choose the proper wave functions for the heavy B_c, and light vector and axial-vector mesons. For the wave function of B_c meson, we adopt the form(see Ref. [2], and references therein) as,

$$\Phi_{B_c}(x) = \frac{i}{\sqrt{2N_c}}\left[(\not{P} + m_{B_c})\gamma_5\phi_{B_c}(x)\right]_{\alpha\beta} . \tag{8}$$

where the distribution amplitude ϕ_{B_c} would be close to $\delta(x - m_c/m_{B_c})$ in the non-relativistic limit because of the fact that B_c meson embraces two heavy quarks. We therefore adopt the non-relativistic approximation form for ϕ_{B_c} as [27, 28],

$$\phi_{B_c}(x) = \frac{f_{B_c}}{2\sqrt{2N_c}}\delta(x - m_c/m_{B_c}) , \tag{9}$$

where f_{B_c} and N_c are the decay constant of B_c meson and the color number, respectively.

For the wave functions of vector and axial-vector mesons, one longitudinal(L) and two transverse(T) polarizations are involved, and can be written as,

$$\Phi_V^L(x) = \frac{1}{\sqrt{2N_c}}\left\{m_V \not{\epsilon}_V^{*L}\phi_V(x) + \not{\epsilon}_V^{*L}\not{P}\phi_V^t(x) + m_V\phi_V^s(x)\right\}_{\alpha\beta} , \tag{10}$$

$$\Phi_V^T(x) = \frac{1}{\sqrt{2N_c}}\left\{m_V \not{\epsilon}_V^{*T}\phi_V^v(x) + \not{\epsilon}_V^{*T}\not{P}\phi_V^T(x) + m_V i\epsilon_{\mu\nu\rho\sigma}\gamma_5\gamma^\mu\epsilon_T^{*\nu}n^\rho v^\sigma\phi_V^a(x)\right\}_{\alpha\beta} , \tag{11}$$

$$\Phi_A^L(x) = \frac{1}{\sqrt{2N_c}}\gamma_5\left\{m_A \not{\epsilon}_A^{*L}\phi_A(x) + \not{\epsilon}_A^{*L}\not{P}\phi_A^t(x) + m_A\phi_A^s(x)\right\}_{\alpha\beta} , \tag{12}$$

$$\Phi_A^T(x) = \frac{1}{\sqrt{2N_c}}\gamma_5\left\{m_A \not{\epsilon}_A^{*T}\phi_A^v(x) + \not{\epsilon}_A^{*T}\not{P}\phi_A^T(x) + m_A i\epsilon_{\mu\nu\rho\sigma}\gamma_5\gamma^\mu\epsilon_T^{*\nu}n^\rho v^\sigma\phi_A^a(x)\right\}_{\alpha\beta} , \tag{13}$$

where $\epsilon^{L,T}_{V(A)}$ denotes the longitudinal and transverse polarization vectors of vector(axial-vector) meson, satisfying $P \cdot \epsilon = 0$ in each polarization, x denotes the momentum fraction carried by quark in the meson, and $n = (1, 0, \mathbf{0}_T)$ and $v = (0, 1, \mathbf{0}_T)$ are dimensionless light-like unit vectors. We here adopt the convention $\epsilon^{0123} = 1$ for the Levi-Civita tensor $\epsilon^{\mu\nu\alpha\beta}$.

The twist-2 distribution amplitudes for the longitudinally and tranversely polarized vector meson can be parameterized as:

$$\phi_V(x) = \frac{3f_V}{\sqrt{2N_c}} x(1-x)\left[1 + 3a^{||}_{1V}(2x-1) + a^{||}_{2V}\frac{3}{2}(5(2x-1)^2-1)\right], \tag{14}$$

$$\phi^T_V(x) = \frac{3f^T_V}{\sqrt{2N_c}} x(1-x)\left[1 + 3a^{\perp}_{1V}(2x-1) + a^{\perp}_{2V}\frac{3}{2}(5(2x-1)^2-1)\right], \tag{15}$$

Here f_V and f^T_V are the decay constants of the vector meson with longitudinal and tranverse polarization, respectively.

The Gegenbauer moments have been studied extensively in the literatures [29, 30], here we adopt the following values from the recent updates [31–33]:

$$a^{||}_{1K^*} = 0.03 \pm 0.02, a^{||}_{2K^*} = 0.11 \pm 0.09, a^{||}_{2\rho} = a^{||}_{2\omega} = 0.15 \pm 0.07, a^{||}_{2\phi} = 0.18 \pm 0.08\ ; \tag{16}$$

$$a^{\perp}_{1K^*} = 0.04 \pm 0.03, a^{\perp}_{2K^*} = 0.10 \pm 0.08, a^{\perp}_{2\rho} = a^{\perp}_{2\omega} = 0.14 \pm 0.06, a^{\perp}_{2\phi} = 0.14 \pm 0.07\ . \tag{17}$$

The asymptotic forms of the twist-3 distribution amplitudes $\phi^{t,s}_V$ and $\phi^{v,a}_V$ are [10]:

$$\phi^t_V(x) = \frac{3f^T_V}{2\sqrt{2N_c}}(2x-1)^2, \qquad \phi^s_V(x) = -\frac{3f^T_V}{2\sqrt{2N_c}}(2x-1)\ , \tag{18}$$

$$\phi^v_V(x) = \frac{3f_V}{8\sqrt{2N_c}}(1+(2x-1)^2), \qquad \phi^a_V(x) = -\frac{3f_V}{4\sqrt{2N_c}}(2x-1). \tag{19}$$

The twist-2 distribution amplitudes for the longitudinally and trasversely polarized axial-vector ${}^3P_1$ and ${}^1P_1$ mesons can be parameterized as [19, 24]:

$$\phi_A(x) = \frac{3f}{\sqrt{2N_c}} x(1-x)\left[a^{||}_{0A} + 3a^{||}_{1A}(2x-1) + a^{||}_{2A}\frac{3}{2}(5(2x-1)^2-1)\right], \tag{20}$$

$$\phi^T_A(x) = \frac{3f}{\sqrt{2N_c}} x(1-x)\left[a^{\perp}_{0A} + 3a^{\perp}_{1A}(2x-1) + a^{\perp}_{2A}\frac{3}{2}(5(2x-1)^2-1)\right], \tag{21}$$

Here, the definition of these distribution amplitudes $\phi_A(x)$ and $\phi^T_A(x)$ satisfy the following relations:

$$\int_0^1 \phi_{^3P_1}(x) = \frac{f_{^3P_1}}{2\sqrt{2N_c}}, \qquad \int_0^1 \phi^T_{^3P_1}(x) = a^{\perp}_{0^3P_1}\frac{f_{^3P_1}}{2\sqrt{2N_c}}\ ;$$

$$\int_0^1 \phi_{^1P_1}(x) = a^{||}_{0^1P_1}\frac{f_{^1P_1}}{2\sqrt{2N_c}}, \qquad \int_0^1 \phi^T_{^1P_1}(x) = \frac{f_{^1P_1}}{2\sqrt{2N_c}}\ . \tag{22}$$

where $a^{||}_{0^3P_1} = 1$ and $a^{\perp}_{0^1P_1} = 1$ have been used.

As for twist-3 distribution amplitudes for axial-vector meson, we use the following form [24]:

$$\phi^t_A(x) = \frac{3f}{2\sqrt{2N_c}}\left\{a^{\perp}_{0A}(2x-1)^2 + \frac{1}{2}a^{\perp}_{1A}(2x-1)(3(2x-1)^2-1)\right\}, \tag{23}$$

$$\phi^s_A(x) = \frac{3f}{2\sqrt{2N_c}}\frac{d}{dx}\left\{x(1-x)(a^{\perp}_{0A} + a^{\perp}_{1A}(2x-1))\right\}. \tag{24}$$

$$\phi_A^v(x) = \frac{3f}{4\sqrt{2N_c}} \left\{ \frac{1}{2} a_{0A}^{\parallel} (1 + (2x-1)^2) + a_{1A}^{\parallel} (2x-1)^3 \right\}, \tag{25}$$

$$\phi_A^a(x) = \frac{3f}{4\sqrt{2N_c}} \frac{d}{dx} \left\{ x(1-x)(a_{0A}^{\parallel} + a_{1A}^{\parallel}(2x-1)) \right\} . \tag{26}$$

where f is the decay constant. It should be noted that in the above distribution amplitudes of strange axial-vector mesons K_{1A} and K_{1B}, x stands for the momentum fraction carrying by the s quark.

The Gegenbauer moments have been studied extensively in the literatures (see Ref. [19] and references therein), here we adopt the following values:

$$\begin{aligned}
a_{2a_1}^{\parallel} &= -0.02 \pm 0.02; & a_{1a_1}^{\perp} &= -1.04 \pm 0.34; & a_{1b_1}^{\parallel} &= -1.95 \pm 0.35; \\
a_{2f_1}^{\parallel} &= -0.04 \pm 0.03; & a_{1f_1}^{\perp} &= -1.06 \pm 0.36; & a_{1h_1}^{\parallel} &= -2.00 \pm 0.35; \\
a_{2f_8}^{\parallel} &= -0.07 \pm 0.04; & a_{1f_8}^{\perp} &= -1.11 \pm 0.31; & a_{1h_8}^{\parallel} &= -1.95 \pm 0.35; \\
a_{1K_{1A}}^{\parallel} &= 0.00 \pm 0.26; & a_{2K_{1A}}^{\parallel} &= -0.05 \pm 0.03; & a_{0K_{1A}}^{\perp} &= 0.08 \pm 0.09; \\
a_{1K_{1A}}^{\perp} &= -1.08 \pm 0.48; & a_{0K_{1B}}^{\parallel} &= 0.14 \pm 0.15; & a_{1K_{1B}}^{\parallel} &= -1.95 \pm 0.45; \\
a_{2K_{1B}}^{\parallel} &= 0.02 \pm 0.10; & a_{1K_{1B}}^{\perp} &= 0.17 \pm 0.22. & &
\end{aligned} \tag{27}$$

D. Formalism of pQCD approach

Since the b quark is rather heavy, we work in the frame with the B_c meson at rest, i.e., with the B_c meson momentum $P_1 = (m_{B_c}/\sqrt{2})(1, 1, \mathbf{0}_T)$ in the light-cone coordinates. For the non-leptonic charmless $B_c \to M_2 M_3$[2] decays, assuming that the M_2 (M_3) meson moves in the plus (minus) z direction carrying the momentum P_2 (P_3) and the polarization vector ϵ_2 (ϵ_3). Then the two final state meson momenta can be written as

$$P_2 = \frac{m_{B_c}}{\sqrt{2}}(1 - r_3^2, r_2^2, \mathbf{0}_T), \quad P_3 = \frac{m_{B_c}}{\sqrt{2}}(r_3^2, 1 - r_2^2, \mathbf{0}_T), \tag{28}$$

respectively, where $r_2 = m_2/m_{B_c}$, $r_3 = m_3/m_{B_c}$ with $m_2 = m_{M_2}$ and $m_3 = m_{M_3}$. The longitudinal polarization vectors, ϵ_2^L and ϵ_3^L, can be given by

$$\epsilon_2^L = \frac{m_{B_c}}{\sqrt{2}m_2}(1 - r_3^2, -r_2^2, \mathbf{0}_T), \quad \epsilon_3^L = \frac{m_{B_c}}{\sqrt{2}m_3}(-r_3^2, 1 - r_2^2, \mathbf{0}_T). \tag{29}$$

And the transverse ones are parameterized as $\epsilon_2^T = (0, 0, 1_T)$, and $\epsilon_3^T = (0, 0, 1_T)$. Putting the (light) quark momenta in B_c, M_2 and M_3 mesons as k_1, k_2, and k_3, respectively, we can choose

$$k_1 = (x_1 P_1^+, 0, \mathbf{k}_{1T}), \quad k_2 = (x_2 P_2^+, 0, \mathbf{k}_{2T}), \quad k_3 = (0, x_3 P_3^-, \mathbf{k}_{3T}). \tag{30}$$

Then, for $B_c \to M_2 M_3$ decays, the integration over k_1^-, k_2^-, and k_3^+ will conceptually lead to the decay amplitudes in the pQCD approach,

$$\begin{aligned}
\mathcal{A}(B_c \to M_2 M_3) \sim & \int dx_1 dx_2 dx_3 b_1 db_1 b_2 db_2 b_3 db_3 \\
& \cdot \mathrm{Tr}\left[C(t) \Phi_{B_c}(x_1, b_1) \Phi_{M_2}(x_2, b_2) \Phi_{M_3}(x_3, b_3) H(x_i, b_i, t) S_t(x_i)\, e^{-S(t)} \right] .
\end{aligned} \tag{31}$$

[2] For the sake of simplicity, in the following, we will use M_2 and M_3 to denote the final state mesons respectively, unless otherwise stated.

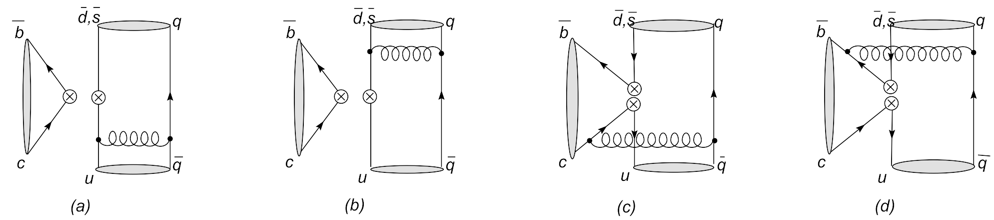

FIG. 1: Typical Feynman diagrams for charmless hadronic $B_c \to VA, AA$ decays.

where b_i is the conjugate space coordinate of k_{iT}, and t is the largest energy scale in function $H(x_i, b_i, t)$. The large logarithms $\ln(m_W/t)$ are included in the Wilson coefficients $C(t)$. The large double logarithms ($\ln^2 x_i$) are summed by the threshold resummation [34], and they lead to $S_t(x_i)$ which smears the endpoint singularities on x_i. The last term, $e^{-S(t)}$, is the Sudakov form factor which suppresses the soft dynamics effectively [35]. Thus it makes the perturbative calculation of the hard part H applicable at intermediate scale, i.e., m_{B_c} scale. We will calculate analytically the function $H(x_i, b_i, t)$ for the considered decays at leading order in α_s expansion and give the convoluted amplitudes in next section.

III. PERTURBATIVE CALCULATIONS IN PQCD APPROACH

There are three kinds of polarizations of a vector or axial-vector meson, namely, longitudinal (L), normal (N), and transverse (T). Similar to the pure annihilation type $B_c \to VV$ decays [2], the amplitudes for a B_c meson decaying into one vector and one axial-vector meson or two axial-vector mesons are also characterized by the polarization states of these vector and axial-vector mesons. In terms of helicities, the decay amplitudes $\mathcal{M}^{(\sigma)}$ for $B_c \to M_2(P_2, \epsilon_2^*) M_3(P_3, \epsilon_3^*)$ decays can be generally described by

$$\begin{aligned}
\mathcal{M}^{(\sigma)} &= \epsilon_{2\mu}^*(\sigma)\epsilon_{3\nu}^*(\sigma)\left[a\, g^{\mu\nu} + \frac{b}{m_2 m_3} P_1^\mu P_1^\nu + i\frac{c}{m_2 m_3}\epsilon^{\mu\nu\alpha\beta} P_{2\alpha} P_{3\beta}\right] , \\
&\equiv m_{B_c}^2 \mathcal{M}_L + m_{B_c}^2 \mathcal{M}_N \epsilon_2^*(\sigma = T)\cdot\epsilon_3^*(\sigma = T) \\
&\quad + i\mathcal{M}_T \epsilon^{\alpha\beta\gamma\rho}\epsilon_{2\alpha}^*(\sigma)\epsilon_{3\beta}^*(\sigma) P_{2\gamma} P_{3\rho} ,
\end{aligned} \tag{32}$$

where the superscript σ denotes the helicity states of one vector and one axial-vector meson or two axial-vector mesons with $L(T)$ standing for the longitudinal (transverse) component. And the definitions of the amplitudes $\mathcal{M}_i (i = L, N, T)$ in terms of the Lorentz-invariant amplitudes a, b and c are

$$\begin{aligned}
m_{B_c}^2\, \mathcal{M}_L &= a\, \epsilon_2^*(L)\cdot\epsilon_3^*(L) + \frac{b}{m_2 m_3}\epsilon_2^*(L)\cdot P_3\, \epsilon_3^*(L)\cdot P_2 , \\
m_{B_c}^2\, \mathcal{M}_N &= a , \\
m_{B_c}^2\, \mathcal{M}_T &= \frac{c}{r_2\, r_3} .
\end{aligned} \tag{33}$$

We therefore will evaluate the helicity amplitudes $\mathcal{M}_L, \mathcal{M}_N, \mathcal{M}_T$ based on the pQCD factorization approach, respectively.

In the following we will present analytically the factorization formulas for sixty two charmless hadronic $B_c \to AV/VA, AA$ decays. From the effective Hamiltonian (1), there are four types of diagrams contributing to these considered decays as illustrated in Fig. 1 with single $(V-A)(V-A)$ currents. From the first two diagrams (a) and (b) in Fig. 1, by perturbative QCD calculations,

we can obtain the Feynman decay amplitudes for factorizable annihilation contributions for $B_c \to AV$, VA, AA as the following sequence,

$$\begin{aligned}
F^{L}_{fa}(AV) &= -8\pi C_F m^2_{B_c} \int_0^1 dx_2 dx_3 \int_0^\infty b_2 db_2 b_3 db_3 \\
&\times \Big\{ \big[x_2 \phi_A(x_2)\phi_V(x_3) - 2r_2^A r_3^V \left((x_2+1)\phi^s_A(x_2) + (x_2-1)\phi^t_A(x_2) \right) \\
&\times \phi^s_V(x_3) \big] E_{fa}(t_a) h_{fa}(1-x_3, x_2, b_3, b_2) + E_{fa}(t_b) h_{fa}(x_2, 1-x_3, b_2, b_3) \\
&\times \big[(x_3-1)\phi_A(x_2)\phi_V(x_3) - 2r_2^A r_3^V \phi^s_A(x_2) \left((x_3-2)\phi^s_V(x_3) - x_3 \phi^t_V(x_3) \right) \big] \Big\} \ , \qquad (34)
\end{aligned}$$

$$\begin{aligned}
F^{N}_{fa}(AV) &= -8\pi C_F m^2_{B_c} \int_0^1 dx_2 dx_3 \int_0^\infty b_2 db_2 b_3 db_3 \, r_2^A r_3^V \\
&\times \{ h_{fa}(1-x_3, x_2, b_3, b_2) E_{fa}(t_a) \left[(x_2+1)(\phi^a_A(x_2)\phi^a_V(x_3) + \phi^v_A(x_2)\phi^v_V(x_3)) \right. \\
&\left. + (x_2-1)(\phi^v_A(x_2)\phi^a_V(x_3) + \phi^a_A(x_2)\phi^v_V(x_3)) \right] \\
&+ \left[(x_3-2)(\phi^a_A(x_2)\phi^a_V(x_3) + \phi^v_A(x_2)\phi^v_V(x_3)) - x_3 (\phi^a_A(x_2)\phi^v_V(x_3) + \phi^v_A(x_2)\phi^a_V(x_3)) \right] \\
&\times E_{fa}(t_b) h_{fa}(x_2, 1-x_3, b_2, b_3) \} \qquad (35)
\end{aligned}$$

$$\begin{aligned}
F^{T}_{fa}(AV) &= -16\pi C_F m^2_{B_c} \int_0^1 dx_2 dx_3 \int_0^\infty b_2 db_2 b_3 db_3 \, r_2^A r_3^V \\
&\times \{ h_{fa}(1-x_3, x_2, b_3, b_2) E_{fa}(t_a) \left[(x_2+1)(\phi^a_A(x_2)\phi^v_V(x_3) + \phi^v_A(x_2)\phi^a_V(x_3)) \right. \\
&\left. + (x_2-1)(\phi^a_A(x_2)\phi^a_V(x_3) + \phi^v_A(x_2)\phi^v_V(x_3)) \right] \\
&+ \left[(x_3-2)(\phi^a_A(x_2)\phi^v_V(x_3) + \phi^v_A(x_2)\phi^a_V(x_3)) - x_3 (\phi^a_A(x_2)\phi^a_V(x_3) + \phi^v_A(x_2)\phi^v_V(x_3)) \right] \\
&\times E_{fa}(t_b) \, h_{fa}(x_2, 1-x_3, b_2, b_3) \} \qquad (36)
\end{aligned}$$

$$\begin{aligned}
F^{L}_{fa}(VA) &= -8\pi C_F m^2_{B_c} \int_0^1 dx_2 dx_3 \int_0^\infty b_2 db_2 b_3 db_3 \\
&\times \Big\{ \big[x_2 \phi_V(x_2)\phi_A(x_3) + 2r_2^V r_3^A \left((x_2+1)\phi^s_V(x_2) + (x_2-1)\phi^t_V(x_2) \right) \\
&\times \phi^s_A(x_3) \big] E_{fa}(t_a) h_{fa}(1-x_3, x_2, b_3, b_2) + E_{fa}(t_b) h_{fa}(x_2, 1-x_3, b_2, b_3) \\
&\times \big[(x_3-1)\phi_V(x_2)\phi_A(x_3) + 2r_2^V r_3^A \phi^s_V(x_2) \left((x_3-2)\phi^s_A(x_3) - x_3 \phi^t_A(x_3) \right) \big] \Big\} \ , \qquad (37)
\end{aligned}$$

$$\begin{aligned}
F^{N}_{fa}(VA) &= -8\pi C_F m^2_{B_c} \int_0^1 dx_2 dx_3 \int_0^\infty b_2 db_2 b_3 db_3 \, r_2^V r_3^A \\
&\times \{ h_{fa}(1-x_3, x_2, b_3, b_2) E_{fa}(t_a) \left[(x_2+1)(\phi^a_V(x_2)\phi^a_A(x_3) + \phi^v_V(x_2)\phi^v_A(x_3)) \right. \\
&\left. + (x_2-1)(\phi^v_V(x_2)\phi^a_A(x_3) + \phi^a_V(x_2)\phi^v_A(x_3)) \right] \\
&+ \left[(x_3-2)(\phi^a_V(x_2)\phi^a_A(x_3) + \phi^v_V(x_2)\phi^v_A(x_3)) - x_3 (\phi^a_V(x_2)\phi^v_A(x_3) + \phi^v_V(x_2)\phi^a_A(x_3)) \right] \\
&\times E_{fa}(t_b) h_{fa}(x_2, 1-x_3, b_2, b_3) \} \ , \qquad (38)
\end{aligned}$$

$$\begin{aligned}
F^{T}_{fa}(VA) &= -16\pi C_F m^2_{B_c} \int_0^1 dx_2 dx_3 \int_0^\infty b_2 db_2 b_3 db_3 \, r_2^V r_3^A \\
&\times \{ h_{fa}(1-x_3, x_2, b_3, b_2) E_{fa}(t_a) \left[(x_2+1)(\phi^a_V(x_2)\phi^v_A(x_3) + \phi^v_V(x_2)\phi^a_A(x_3)) \right. \\
&\left. + (x_2-1)(\phi^a_V(x_2)\phi^a_A(x_3) + \phi^v_V(x_2)\phi^v_A(x_3)) \right] \\
&+ \left[(x_3-2)(\phi^a_V(x_2)\phi^v_A(x_3) + \phi^v_V(x_2)\phi^a_A(x_3)) - x_3 (\phi^a_V(x_2)\phi^a_A(x_3) + \phi^v_V(x_2)\phi^v_A(x_3)) \right] \\
&\times E_{fa}(t_b) \, h_{fa}(x_2, 1-x_3, b_2, b_3) \} \ , \qquad (39)
\end{aligned}$$

$$\begin{aligned}
F_{fa}^{L}(AA) &= 8\pi C_F m_{B_c}^2 \int_0^1 dx_2 dx_3 \int_0^\infty b_2 db_2 b_3 db_3 \\
&\times \left\{ \left[x_2 \phi_2(x_2)\phi_3(x_3) + 2r_2^A r_3^A \left((x_2+1)\phi_2^s(x_2) + (x_2-1)\phi_2^t(x_2) \right) \right.\right. \\
&\left.\times \phi_3^s(x_3) \right] E_{fa}(t_a) h_{fa}(1-x_3, x_2, b_3, b_2) + E_{fa}(t_b) h_{fa}(x_2, 1-x_3, b_2, b_3) \\
&\left.\times \left[(x_3-1)\phi_2(x_2)\phi_3(x_3) + 2r_2^A r_3^A \phi_2^s(x_2) \left((x_3-2)\phi_3^s(x_3) - x_3\phi_3^t(x_3) \right) \right] \right\} , \qquad (40) \\
F_{fa}^{N}(AA) &= 8\pi C_F m_{B_c}^2 \int_0^1 dx_2 dx_3 \int_0^\infty b_2 db_2 b_3 db_3 \, r_2^A r_3^A \\
&\times \{ h_{fa}(1-x_3, x_2, b_3, b_2) E_{fa}(t_a) \left[(x_2+1)(\phi_2^a(x_2)\phi_3^a(x_3) + \phi_2^v(x_2)\phi_3^v(x_3)) \right. \\
&\left. +(x_2-1)(\phi_2^v(x_2)\phi_3^a(x_3) + \phi_2^a(x_2)\phi_3^v(x_3)) \right] \\
&+ \left[(x_3-2)(\phi_2^a(x_2)\phi_3^a(x_3) + \phi_2^v(x_2)\phi_3^v(x_3)) - x_3 \left(\phi_2^a(x_2)\phi_3^v(x_3) + \phi_2^v(x_2)\phi_3^a(x_3) \right) \right] \\
&\times E_{fa}(t_b) h_{fa}(x_2, 1-x_3, b_2, b_3) \} , \qquad (41) \\
F_{fa}^{T}(AA) &= 16\pi C_F m_{B_c}^2 \int_0^1 dx_2 dx_3 \int_0^\infty b_2 db_2 b_3 db_3 \, r_2^A r_3^A \\
&\times \{ h_{fa}(1-x_3, x_2, b_3, b_2) E_{fa}(t_a) \left[(x_2+1)(\phi_2^a(x_2)\phi_3^v(x_3) + \phi_2^v(x_2)\phi_3^a(x_3)) \right. \\
&\left. +(x_2-1)(\phi_2^a(x_2)\phi_3^a(x_3) + \phi_2^v(x_2)\phi_3^v(x_3)) \right] \\
&+ \left[(x_3-2)(\phi_2^a(x_2)\phi_3^v(x_3) + \phi_2^v(x_2)\phi_3^a(x_3)) - x_3 \left(\phi_2^a(x_2)\phi_3^a(x_3) + \phi_2^v(x_2)\phi_3^v(x_3) \right) \right] \\
&\times E_{fa}(t_b) \, h_{fa}(x_2, 1-x_3, b_2, b_3) \} , \qquad (42)
\end{aligned}$$

where the superscripts V and A in the formulas express the types of mesons involved in the considered decays, the subscripts fa and na (to be shown below) are the abbreviations of factorizable annihilation and nonfactorizable annihilation respectively, and $C_F = 4/3$ is a color factor. Moreover, the terms proportional to $r_{2(3)}^2$ can not change the results significantly and they have been neglected safely because the values of $r_{2(3)}^2$ are numerically small: $r_{2(3)}^2 < 5\%$. For the function h_{fa}, the scales t_i, and $E_{fa}(t)$, we use the expressions as given in Appendix B of Ref. [2].

For the nonfactorizable diagrams (c) and (d) in Fig. 1, all three meson wave functions are involved. The integration of b_3 can be performed using δ function $\delta(b_3 - b_2)$, leaving only integration of b_1 and b_2. The corresponding decay amplitudes are

$$\begin{aligned}
M_{na}^{L}(AV) &= -\frac{16\sqrt{6}}{3}\pi C_F m_{B_c}^2 \int_0^1 dx_2 \, dx_3 \int_0^\infty b_1 db_1 b_2 db_2 \\
&\times \left\{ E_{na}(t_c) \left[(r_c - x_3 + 1)\phi_A(x_2)\phi_V(x_3) - r_2^A r_3^V \left(\phi_A^s(x_2)((3r_c + x_2 - x_3 + 1) \right.\right.\right. \\
&\times \phi_V^s(x_3) - (r_c - x_2 - x_3 + 1)\phi_V^t(x_3)) + \phi_A^t(x_2)((r_c - x_2 - x_3 + 1)\phi_V^s(x_3) \\
&\left.\left. +(r_c - x_2 + x_3 - 1)\phi_V^t(x_3)))\right) \right] h_{na}^c(x_2, x_3, b_1, b_2) - h_{na}^d(x_2, x_3, b_1, b_2) E_{na}(t_d) \\
&\times \left[(r_b + r_c + x_2 - 1)\phi_A(x_2)\phi_V(x_3) - r_2^A r_3^V \left(\phi_A^s(x_2)((4r_b + r_c + x_2 - x_3 - 1) \right.\right. \\
&\times \phi_V^s(x_3) - (r_c + x_2 + x_3 - 1)\phi_V^t(x_3)) + \phi_A^t(x_2)((r_c + x_2 + x_3 - 1)\phi_V^s(x_3) \\
&\left.\left.\left. -(r_c + x_2 - x_3 - 1)\phi_V^t(x_3)))\right) \right] \right\} , \qquad (43) \\
M_{na}^{N}(AV) &= -\frac{32\sqrt{6}}{3}\pi C_F m_{B_c}^2 \int_0^1 dx_2 \, dx_3 \int_0^\infty b_1 db_1 b_2 db_2 \, r_2^A r_3^V \\
&\times \left\{ r_c \left[\phi_A^a(x_2)\phi_V^a(x_3) + \phi_A^v(x_2)\phi_V^v(x_3) \right] E_{na}(t_c) h_{na}^c(x_2, x_3, b_1, b_2) \right. \\
&\left. -r_b \left[\phi_A^a(x_2)\phi_A^a(x_3) + \phi_A^v(x_2)\phi_V^v(x_3) \right] E_{na}(t_d) h_{na}^d(x_2, x_3, b_1, b_2) \right\} , \qquad (44)
\end{aligned}$$

$$
\begin{aligned}
M_{na}^{T}(AV) \;=\; & -\frac{64\sqrt{6}}{3}\pi C_F m_{B_c}^2 \int_0^1 dx_2\, dx_3 \int_0^\infty b_1 db_1 b_2 db_2\, r_2^A r_3^V \\
& \times \{ r_c \left[\phi_A^a(x_2)\phi_V^v(x_3) + \phi_A^v(x_2)\phi_V^a(x_3)\right] E_{na}(t_c) h_{na}^c(x_2,x_3,b_1,b_2) \\
& - r_b \left[\phi_A^a(x_2)\phi_V^v(x_3) + \phi_A^v(x_2)\phi_V^a(x_3)\right] E_{na}(t_d) h_{na}^d(x_2,x_3,b_1,b_2) \Big\} \;. \qquad (45)
\end{aligned}
$$

$$
\begin{aligned}
M_{na}^{L}(VA) \;=\; & -\frac{16\sqrt{6}}{3}\pi C_F m_{B_c}^2 \int_0^1 dx_2\, dx_3 \int_0^\infty b_1 db_1 b_2 db_2 \\
& \times \big\{ E_{na}(t_c) \big[(r_c - x_3 + 1)\phi_V(x_2)\phi_A(x_3) + r_2^V r_3^A \left(\phi_V^s(x_2)((3r_c + x_2 - x_3 + 1)\right. \\
& \times \phi_A^s(x_3) - (r_c - x_2 - x_3 + 1)\phi_A^t(x_3)) + \phi_V^t(x_2)((r_c - x_2 - x_3 + 1)\phi_A^s(x_3) \\
& + (r_c - x_2 + x_3 - 1)\phi_A^t(x_3)))\big] h_{na}^c(x_2,x_3,b_1,b_2) - h_{na}^d(x_2,x_3,b_1,b_2) E_{na}(t_d) \\
& \times \big[(r_b + r_c + x_2 - 1)\phi_V(x_2)\phi_A(x_3) + r_2^V r_3^A \left(\phi_V^s(x_2)((4r_b + r_c + x_2 - x_3 - 1)\right. \\
& \times \phi_A^s(x_3) - (r_c + x_2 + x_3 - 1)\phi_A^T(x_3)) + \phi_V^t(x_2)((r_c + x_2 + x_3 - 1)\phi_A^s(x_3) \\
& - (r_c + x_2 - x_3 - 1)\phi_A^t(x_3)))\big]\big\} \;, \qquad (46)
\end{aligned}
$$

$$
\begin{aligned}
M_{na}^{N}(VA) \;=\; & -\frac{32\sqrt{6}}{3}\pi C_F m_{B_c}^2 \int_0^1 dx_2\, dx_3 \int_0^\infty b_1 db_1 b_2 db_2\, r_2^V r_3^A \\
& \times \{ r_c \left[\phi_V^a(x_2)\phi_A^a(x_3) + \phi_V^v(x_2)\phi_A^v(x_3)\right] E_{na}(t_c) h_{na}^c(x_2,x_3,b_1,b_2) \\
& - r_b \left[\phi_V^a(x_2)\phi_A^a(x_3) + \phi_V^v(x_2)\phi_A^v(x_3)\right] E_{na}(t_d) h_{na}^d(x_2,x_3,b_1,b_2) \Big\} \;, \qquad (47)
\end{aligned}
$$

$$
\begin{aligned}
M_{na}^{T}(VA) \;=\; & -\frac{64\sqrt{6}}{3}\pi C_F m_{B_c}^2 \int_0^1 dx_2\, dx_3 \int_0^\infty b_1 db_1 b_2 db_2\, r_2^V r_3^A \\
& \times \{ r_c \left[\phi_V^a(x_2)\phi_A^v(x_3) + \phi_V^v(x_2)\phi_A^a(x_3)\right] E_{na}(t_c) h_{na}^c(x_2,x_3,b_1,b_2) \\
& - r_b \left[\phi_V^a(x_2)\phi_A^v(x_3) + \phi_V^v(x_2)\phi_A^a(x_3)\right] E_{na}(t_d) h_{na}^d(x_2,x_3,b_1,b_2) \Big\} \;. \qquad (48)
\end{aligned}
$$

$$
\begin{aligned}
M_{na}^{L}(AA) \;=\; & \frac{16\sqrt{6}}{3}\pi C_F m_{B_c}^2 \int_0^1 dx_2\, dx_3 \int_0^\infty b_1 db_1 b_2 db_2 \\
& \times \big\{ E_{na}(t_c) \big[(r_c - x_3 + 1)\phi_2(x_2)\phi_3(x_3) + r_2^A r_3^A \left(\phi_2^s(x_2)((3r_c + x_2 - x_3 + 1)\right. \\
& \times \phi_3^s(x_3) - (r_c - x_2 - x_3 + 1)\phi_3^t(x_3)) + \phi_2^t(x_2)((r_c - x_2 - x_3 + 1)\phi_3^s(x_3) \\
& + (r_c - x_2 + x_3 - 1)\phi_3^t(x_3)))\big] h_{na}^c(x_2,x_3,b_1,b_2) - h_{na}^d(x_2,x_3,b_1,b_2) E_{na}(t_d) \\
& \times \big[(r_b + r_c + x_2 - 1)\phi_2(x_2)\phi_3(x_3) + r_2^A r_3^A \left(\phi_2^s(x_2)((4r_b + r_c + x_2 - x_3 - 1)\right. \\
& \times \phi_3^s(x_3) - (r_c + x_2 + x_3 - 1)\phi_3^t(x_3)) + \phi_2^t(x_2)((r_c + x_2 + x_3 - 1)\phi_3^s(x_3) \\
& - (r_c + x_2 - x_3 - 1)\phi_3^t(x_3)))\big]\big\} \;, \qquad (49)
\end{aligned}
$$

$$
\begin{aligned}
M_{na}^{N}(AA) \;=\; & \frac{32\sqrt{6}}{3}\pi C_F m_{B_c}^2 \int_0^1 dx_2\, dx_3 \int_0^\infty b_1 db_1 b_2 db_2\, r_2^A r_3^A \\
& \times \{ r_c \left[\phi_2^a(x_2)\phi_3^a(x_3) + \phi_2^v(x_2)\phi_3^v(x_3)\right] E_{na}(t_c) h_{na}^c(x_2,x_3,b_1,b_2) \\
& - r_b \left[\phi_2^a(x_2)\phi_3^a(x_3) + \phi_2^v(x_2)\phi_3^v(x_3)\right] E_{na}(t_d) h_{na}^d(x_2,x_3,b_1,b_2) \Big\} \;, \qquad (50)
\end{aligned}
$$

$$
\begin{aligned}
M_{na}^{T}(AA) \;=\; & \frac{64\sqrt{6}}{3}\pi C_F m_{B_c}^2 \int_0^1 dx_2\, dx_3 \int_0^\infty b_1 db_1 b_2 db_2\, r_2^A r_3^A \\
& \times \{ r_c \left[\phi_2^a(x_2)\phi_3^v(x_3) + \phi_2^v(x_2)\phi_3^a(x_3)\right] E_{na}(t_c) h_{na}^c(x_2,x_3,b_1,b_2) \\
& - r_b \left[\phi_2^a(x_2)\phi_3^v(x_3) + \phi_2^v(x_2)\phi_3^a(x_3)\right] E_{na}(t_d) h_{na}^d(x_2,x_3,b_1,b_2) \Big\} \;. \qquad (51)
\end{aligned}
$$

where $r_b = m_b/m_{B_c}$, $r_c = m_c/m_{B_c}$, and $r_b + r_c \approx 1$ for B_c meson.

There are three kinds of polarizations in these $B_c \to VA, AA$ decays, namely, longitudinal (L), normal (N) and transverse (T). The decay amplitudes are classified accordingly, with $H = L, N, T$. From the effective Hamiltonian (1), based on Eqs. (34-51), we can combine all contributions to these considered decays and obtain the total decay amplitude generally as,

$$\mathcal{M}^H(B_c \to M_2 M_3) \;=\; V_{cb}^* V_{uD} \left\{ f_{B_c} F_{fa;H}^{M_2 M_3} a_1 + M_{na;H}^{M_2 M_3} C_1 \right\} , \tag{52}$$

where $a_1 = C_1/3 + C_2$. Then we can write down the total decay amplitudes for sixty two charmless two-body nonleptonic B_c meson decays into final states involving one vector and one axial-vector meson (VA) or two axial-vector mesons(AA) one by one.

1. $B_c \to VA/AV$ decay modes

(i) For $\Delta S = 0$ processes,

$$\begin{aligned}\sqrt{2}\mathcal{M}^H(B_c \to \rho^+ a_1^0) \;&=\; V_{cb}^* V_{ud} \left\{ \left[f_{B_c} F_{fa;H}^{\rho a_{1u}^0} a_1 + M_{na;H}^{\rho a_{1u}^0} C_1 \right] \right.\\ &\quad \left. - \left[f_{B_c} F_{fa;H}^{a_{1d}^0 \rho} a_1 + M_{na;H}^{a_{1d}^0 \rho} C_1 \right] \right\} ,\end{aligned} \tag{53}$$

$$\begin{aligned}\sqrt{2}\mathcal{M}^H(B_c \to a_1^+ \rho^0) \;&=\; -\sqrt{2}\mathcal{M}^H(B_c \to \rho^+ a_1^0)\\ &=\; V_{cb}^* V_{ud} \left\{ \left[f_{B_c} F_{fa;H}^{a_1^+ \rho_u^0} a_1 + M_{na;H}^{a_1^+ \rho_u^0} C_1 \right] \right.\\ &\quad \left. - \left[f_{B_c} F_{fa;H}^{\rho_d^0 a_1^+} a_1 + M_{na;H}^{\rho_d^0 a_1^+} C_1 \right] \right\} ,\end{aligned} \tag{54}$$

$$\begin{aligned}\sqrt{2}\mathcal{M}^H(B_c \to a_1^+ \omega) \;&=\; V_{cb}^* V_{ud} \left\{ \left[f_{B_c} F_{fa;H}^{a_1^+ \omega_u} a_1 + M_{na;H}^{a_1^+ \omega_u} C_1 \right] \right.\\ &\quad \left. + \left[f_{B_c} F_{fa;H}^{\omega_d a_1^+} a_1 + M_{na;H}^{\omega_d a_1^+} C_1 \right] \right\} ,\end{aligned} \tag{55}$$

$$\begin{aligned}\sqrt{2}\mathcal{M}^H(B_c \to \rho^+ b_1^0) \;&=\; V_{cb}^* V_{ud} \left\{ \left[f_{B_c} F_{fa;H}^{\rho b_{1u}^0} a_1 + M_{na;H}^{\rho b_{1u}^0} C_1 \right] \right.\\ &\quad \left. - \left[f_{B_c} F_{fa;H}^{b_{1d}^0 \rho} a_1 + M_{na;H}^{b_{1d}^0 \rho} C_1 \right] \right\} ,\end{aligned} \tag{56}$$

$$\begin{aligned}\sqrt{2}\mathcal{M}^H(B_c \to b_1^+ \rho^0) \;&=\; -\sqrt{2}\mathcal{M}^H(B_c \to \rho^+ b_1^0)\\ &=\; V_{cb}^* V_{ud} \left\{ \left[f_{B_c} F_{fa;H}^{b_1^+ \rho_u^0} a_1 + M_{na;H}^{b_1^+ \rho_u^0} C_1 \right] \right.\\ &\quad \left. - \left[f_{B_c} F_{fa;H}^{\rho_d^0 b_1^+} a_1 + M_{na;H}^{\rho_d^0 b_1^+} C_1 \right] \right\} ,\end{aligned} \tag{57}$$

$$\begin{aligned}\sqrt{2}\mathcal{M}^H(B_c \to b_1^+ \omega) \;&=\; V_{cb}^* V_{ud} \left\{ \left[f_{B_c} F_{fa;H}^{b_1^+ \omega_u} a_1 + M_{na;H}^{b_1^+ \omega_u} C_1 \right] \right.\\ &\quad \left. + \left[f_{B_c} F_{fa;H}^{\omega_d b_1^+} a_1 + M_{na;H}^{\omega_d b_1^+} C_1 \right] \right\} ,\end{aligned} \tag{58}$$

$$\begin{aligned}\mathcal{M}^H(B_c \to \rho^+ f') \;&=\; V_{cb}^* V_{ud} \left\{ \frac{\cos\theta_3}{\sqrt{3}} \left[f_{B_c} (F_{fa;H}^{\rho f_1^u} + F_{fa;H}^{f_1^d \rho}) a_1 \right.\right.\\ &\quad \left. +(M_{na;H}^{\rho f_1^u} + M_{na;H}^{f_1^d \rho}) C_1 \right] + \frac{\sin\theta_3}{\sqrt{6}} \left[f_{B_c} \right.\\ &\quad \left.\left. \cdot (F_{fa;H}^{\rho f_8^u} + F_{fa;H}^{f_8^d \rho}) a_1 + (M_{na;H}^{\rho f_8^u} + M_{na;H}^{f_8^d \rho}) C_1 \right] \right\} ,\end{aligned} \tag{59}$$

$$\mathcal{M}^H(B_c\to\rho^+f'') = V_{cb}^*V_{ud}\left\{\frac{-\sin\theta_3}{\sqrt{3}}\left[f_{B_c}(F^{\rho f_1^u}_{fa;H}+F^{f_1^d\rho}_{fa;H})a_1 +(M^{\rho f_1^u}_{na;H}+M^{f_1^d\rho}_{na;H})C_1\right]+\frac{\cos\theta_3}{\sqrt{6}}\left[f_{B_c} \cdot(F^{\rho f_8^u}_{fa;H}+F^{f_8^d\rho}_{fa;H})a_1+(M^{\rho f_8^u}_{na;H}+M^{f_8^d\rho}_{na;H})C_1\right]\right\}, \tag{60}$$

$$\mathcal{M}^H(B_c\to\rho^+h') = V_{cb}^*V_{ud}\left\{\frac{\cos\theta_1}{\sqrt{3}}\left[f_{B_c}(F^{\rho h_1^u}_{fa;H}+F^{h_1^d\rho}_{fa;H})a_1 +(M^{\rho h_1^u}_{na;H}+M^{h_1^d\rho}_{na;H})C_1\right]+\frac{\sin\theta_1}{\sqrt{6}}\left[f_{B_c} \cdot(F^{\rho h_8^u}_{fa;H}+F^{h_8^d\rho}_{fa;H})a_1+(M^{\rho h_8^u}_{na;H}+M^{h_8^d\rho}_{na;H})C_1\right]\right\}, \tag{61}$$

$$\mathcal{M}^H(B_c\to\rho^+h'') = V_{cb}^*V_{ud}\left\{\frac{-\sin\theta_1}{\sqrt{3}}\left[f_{B_c}(F^{\rho h_1^u}_{fa;H}+F^{h_1^d\rho}_{fa;H})a_1 +(M^{\rho h_1^u}_{na;H}+M^{h_1^d\rho}_{na;H})C_1\right]+\frac{\cos\theta_1}{\sqrt{6}}\left[f_{B_c} \cdot(F^{\rho h_8^u}_{fa;H}+F^{h_8^d\rho}_{fa;H})a_1+(M^{\rho h_8^u}_{na;H}+M^{h_8^d\rho}_{na;H})C_1\right]\right\}, \tag{62}$$

$$\mathcal{M}^H(B_c\to\overline{K^{*0}}K'^+) = V_{cb}^*V_{ud}\left\{\sin\theta_K\left[f_{B_c}F^{\overline{K^{*0}}K_{1A}}_{fa;H}a_1+M^{\overline{K^{*0}}K_{1A}}_{na;H}C_1\right] +\cos\theta_K\left[f_{B_c}F^{\overline{K^{*0}}K_{1B}}_{fa;H}a_1+M^{\overline{K^{*0}}K_{1B}}_{na;H}C_1\right]\right\}, \tag{63}$$

$$\mathcal{M}^H(B_c\to\overline{K^{*0}}K''^+) = V_{cb}^*V_{ud}\left\{\cos\theta_K\left[f_{B_c}F^{\overline{K^{*0}}K_{1A}}_{fa;H}a_1+M^{\overline{K^{*0}}K_{1A}}_{na;H}C_1\right] -\sin\theta_K\left[f_{B_c}F^{\overline{K^{*0}}K_{1B}}_{fa;H}a_1+M^{\overline{K^{*0}}K_{1B}}_{na;H}C_1\right]\right\}, \tag{64}$$

$$\mathcal{M}^H(B_c\to\overline{K'}^0K^{*+}) = V_{cb}^*V_{ud}\left\{\sin\theta_K\left[f_{B_c}F^{\overline{K^0_{1A}}K^*}_{fa;H}a_1+M^{\overline{K^0_{1A}}K^*}_{na;H}C_1\right] +\cos\theta_K\left[f_{B_c}F^{\overline{K^0_{1B}}K^*}_{fa;H}a_1+M^{\overline{K^0_{1B}}K^*}_{na;H}C_1\right]\right\}, \tag{65}$$

$$\mathcal{M}^H(B_c\to\overline{K''}^0K^{*+}) = V_{cb}^*V_{ud}\left\{\cos\theta_K\left[f_{B_c}F^{\overline{K^0_{1A}}K^*}_{fa;H}a_1+M^{\overline{K^0_{1A}}K^*}_{na;H}C_1\right] -\sin\theta_K\left[f_{B_c}F^{\overline{K^0_{1B}}K^*}_{fa;H}a_1+M^{\overline{K^0_{1B}}K^*}_{na;H}C_1\right]\right\}. \tag{66}$$

(ii) For $\Delta S=1$ processes,

$$\mathcal{M}^H(B_c\to K^{*0}a_1^+) = \sqrt{2}\mathcal{M}^H(B_c\to K^{*+}a_1^0) = V_{cb}^*V_{us}\left\{f_{B_c}F^{K^{*0}a_1^+}_{fa;H}a_1+M^{K^{*0}a_1^+}_{na;H}C_1\right\}, \tag{67}$$

$$\mathcal{M}^H(B_c\to K^{*0}b_1^+) = \sqrt{2}\mathcal{M}^H(B_c\to K^{*+}b_1^0) = V_{cb}^*V_{us}\left\{f_{B_c}F^{K^{*0}b_1^+}_{fa;H}a_1+M^{K^{*0}b_1^+}_{na;H}C_1\right\}, \tag{68}$$

$$\begin{aligned}\mathcal{M}^H(B_c\to K'^0\rho^+) &= \sqrt{2}\mathcal{M}^H(B_c\to K'^+\rho^0)\\ &= V_{cb}^*V_{us}\Big\{\sin\theta_K\Big[f_{B_c}F_{fa;H}^{K_{1A}^0\rho}a_1+M_{na;H}^{K_{1A}^0\rho}C_1\Big]\\ &\quad+\cos\theta_K\Big[f_{B_c}F_{fa;H}^{K_{1B}^0\rho}a_1+M_{na;H}^{K_{1B}^0\rho}C_1\Big]\Big\},\end{aligned}\tag{69}$$

$$\begin{aligned}\mathcal{M}^H(B_c\to K''^0\rho^+) &= \sqrt{2}\mathcal{M}^H(B_c\to K''^+\rho^0)\\ &= V_{cb}^*V_{us}\Big\{\cos\theta_K\Big[f_{B_c}F_{fa;H}^{K_{1A}^0\rho}a_1+M_{na;H}^{K_{1A}^0\rho}C_1\Big]\\ &\quad-\sin\theta_K\Big[f_{B_c}F_{fa;H}^{K_{1B}^0\rho}a_1+M_{na;H}^{K_{1B}^0\rho}C_1\Big]\Big\},\end{aligned}\tag{70}$$

$$\begin{aligned}\sqrt{2}\mathcal{M}^H(B_c\to K'^+\omega) &= V_{cb}^*V_{us}\Big\{\sin\theta_K\Big[f_{B_c}F_{fa;H}^{K_{1A}^0\omega}a_1+M_{na;H}^{K_{1A}^0\omega}C_1\Big]\\ &\quad+\cos\theta_K\Big[f_{B_c}F_{fa;H}^{K_{1B}^0\omega}a_1+M_{na;H}^{K_{1B}^0\omega}C_1\Big]\Big\},\end{aligned}\tag{71}$$

$$\begin{aligned}\sqrt{2}\mathcal{M}^H(B_c\to K''^+\omega) &= V_{cb}^*V_{us}\Big\{\cos\theta_K\Big[f_{B_c}F_{fa;H}^{K_{1A}^0\omega}a_1+M_{na;H}^{K_{1A}^0\omega}C_1\Big]\\ &\quad-\sin\theta_K\Big[f_{B_c}F_{fa;H}^{K_{1B}^0\omega}a_1+M_{na;H}^{K_{1B}^0\omega}C_1\Big]\Big\},\end{aligned}\tag{72}$$

$$\begin{aligned}\mathcal{M}^H(B_c\to K^{*+}f') &= V_{cb}^*V_{us}\Big\{\frac{\cos\theta_3}{\sqrt{3}}\Big[f_{B_c}(F_{fa;H}^{K^*f_1^u}+F_{fa;H}^{f_1^sK^*})a_1\\ &\quad+(M_{na;H}^{K^*f_1^u}+M_{na;H}^{f_1^sK^*})C_1\Big]+\frac{\sin\theta_3}{\sqrt{6}}\,[f_{B_c}\\ &\quad\cdot(F_{fa;H}^{K^*f_8^u}-2F_{fa;H}^{f_8^sK^*})a_1+(M_{na;H}^{K^*f_8^u}-2M_{na;H}^{f_8^sK^*})C_1\Big]\Big\}\ ,\end{aligned}\tag{73}$$

$$\begin{aligned}\mathcal{M}^H(B_c\to K^{*+}f'') &= V_{cb}^*V_{us}\Big\{\frac{-\sin\theta_3}{\sqrt{3}}\Big[f_{B_c}(F_{fa;H}^{K^*f_1^u}+F_{fa;H}^{f_1^sK^*})a_1\\ &\quad+(M_{na;H}^{K^*f_1^u}+M_{na;H}^{f_1^sK^*})C_1\Big]+\frac{\cos\theta_3}{\sqrt{6}}\,[f_{B_c}\\ &\quad\cdot(F_{fa;H}^{K^*f_8^u}-2F_{fa;H}^{f_8^sK^*})a_1+(M_{na;H}^{K^*f_8^u}-2M_{na;H}^{f_8^sK^*})C_1\Big]\Big\}\ ,\end{aligned}\tag{74}$$

$$\begin{aligned}\mathcal{M}^H(B_c\to K^{*+}h') &= V_{cb}^*V_{us}\Big\{\frac{\cos\theta_1}{\sqrt{3}}\Big[f_{B_c}(F_{fa;H}^{K^*h_1^u}+F_{fa;H}^{h_1^sK^*})a_1\\ &\quad+(M_{na;H}^{K^*h_1^u}+M_{na;H}^{h_1^sK^*})C_1\Big]+\frac{\sin\theta_1}{\sqrt{6}}\,[f_{B_c}\\ &\quad\cdot(F_{fa;H}^{K^*h_8^u}-2F_{fa;H}^{h_8^sK^*})a_1+(M_{na;H}^{K^*h_8^u}-2M_{na;H}^{h_8^sK^*})C_1\Big]\Big\}\ ,\end{aligned}\tag{75}$$

$$\begin{aligned}\mathcal{M}^H(B_c\to K^{*+}h'') &= V_{cb}^*V_{us}\Big\{\frac{-\sin\theta_1}{\sqrt{3}}\Big[f_{B_c}(F_{fa;H}^{K^*h_1^u}+F_{fa;H}^{h_1^sK^*})a_1\\ &\quad+(M_{na;H}^{K^*h_1^u}+M_{na;H}^{h_1^sK^*})C_1\Big]+\frac{\cos\theta_1}{\sqrt{6}}\,[f_{B_c}\\ &\quad\cdot(F_{fa;H}^{K^*h_8^u}-2F_{fa;H}^{h_8^sK^*})a_1+(M_{na;H}^{K^*h_8^u}-2M_{na;H}^{h_8^sK^*})C_1\Big]\Big\}\ ,\end{aligned}\tag{76}$$

$$\mathcal{M}^H(B_c \to \phi K'^+) = V_{cb}^* V_{us} \Big\{ \sin\theta_K \Big[f_{B_c} F_{fa;H}^{\phi K_{1A}^0} a_1 + M_{na;H}^{\phi K_{1A}^0} C_1 \Big] + \cos\theta_K \Big[f_{B_c} F_{fa;H}^{\phi K_{1B}^0} a_1 + M_{na;H}^{\phi K_{1B}^0} C_1 \Big] \Big\}, \tag{77}$$

$$\mathcal{M}^H(B_c \to \phi K''^+) = V_{cb}^* V_{us} \Big\{ \cos\theta_K \Big[f_{B_c} F_{fa;H}^{\phi K_{1A}^0} a_1 + M_{na;H}^{\phi K_{1A}^0} C_1 \Big] - \sin\theta_K \Big[f_{B_c} F_{fa;H}^{\phi K_{1B}^0} a_1 + M_{na;H}^{\phi K_{1B}^0} C_1 \Big] \Big\}. \tag{78}$$

2. $B_c \to AA$ decay modes

(i) For $\Delta S = 0$ processes,

$$\sqrt{2}\mathcal{M}^H(B_c \to a_1^+ a_1^0) = V_{cb}^* V_{ud} \Big\{ f_{B_c} (F_{fa;H}^{a_1^+ a_{1u}^0} - F_{fa;H}^{a_{1d}^0 a_1^+}) a_1 + (M_{na;H}^{a_1^+ a_{1u}^0} - M_{na;H}^{a_{1d}^0 a_1^+}) C_1 \Big\}, \tag{79}$$

$$\sqrt{2}\mathcal{M}^H(B_c \to b_1^+ b_1^0) = V_{cb}^* V_{ud} \Big\{ f_{B_c} (F_{fa;H}^{b_1^+ b_{1u}^0} - F_{fa;H}^{b_{1d}^0 b_1^+}) a_1 + (M_{na;H}^{b_1^+ b_{1u}^0} - M_{na;H}^{b_{1d}^0 b_1^+}) C_1 \Big\}, \tag{80}$$

$$\sqrt{2}\mathcal{M}^H(B_c \to a_1^+ b_1^0) = V_{cb}^* V_{ud} \Big\{ f_{B_c} (F_{fa;H}^{a_1^+ b_{1u}^0} - F_{fa;H}^{b_{1d}^0 a_1^+}) a_1 + (M_{na;H}^{a_1^+ b_{1u}^0} - M_{na;H}^{b_{1d}^0 a_1^+}) C_1 \Big\}, \tag{81}$$

$$\sqrt{2}\mathcal{M}^H(B_c \to b_1^+ a_1^0) = V_{cb}^* V_{ud} \Big\{ f_{B_c} (F_{fa;H}^{b_1^+ a_{1u}^0} - F_{fa;H}^{a_{1d}^0 b_1^+}) a_1 + (M_{na;H}^{b_1^+ a_{1u}^0} - M_{na;H}^{a_{1d}^0 b_1^+}) C_1 \Big\}, \tag{82}$$

$$\mathcal{M}^H(B_c \to a_1^+ f') = V_{cb}^* V_{ud} \Big\{ \frac{\cos\theta_3}{\sqrt{3}} [f_{B_c} (F_{fa;H}^{a_1^+ f_1^u} + F_{fa;H}^{f_1^d a_1^+}) a_1 + (M_{na;H}^{a_1^+ f_1^u} + M_{na;H}^{f_1^d a_1^+}) C_1] + \frac{\sin\theta_3}{\sqrt{6}} [f_{B_c} \cdot (F_{fa;H}^{a_1^+ f_8^u} + F_{fa;H}^{f_8^d a_1^+}) a_1 + (M_{na;H}^{a_1^+ f_8^u} + M_{na;H}^{f_8^d a_1^+}) C_1] \Big\}, \tag{83}$$

$$\mathcal{M}^H(B_c \to a_1^+ f'') = V_{cb}^* V_{ud} \Big\{ \frac{-\sin\theta_3}{\sqrt{3}} [f_{B_c} (F_{fa;H}^{a_1^+ f_1^u} + F_{fa;H}^{f_1^d a_1^+}) a_1 + (M_{na;H}^{a_1^+ f_1^u} + M_{na;H}^{f_1^d a_1^+}) C_1] + \frac{\cos\theta_3}{\sqrt{6}} [f_{B_c} \cdot (F_{fa;H}^{a_1^+ f_8^u} + F_{fa;H}^{f_8^d a_1^+}) a_1 + (M_{na;H}^{a_1^+ f_8^u} + M_{na;H}^{f_8^d a_1^+}) C_1] \Big\}, \tag{84}$$

$$\begin{aligned}\mathcal{M}^H(B_c\to b_1^+ f') &= V_{cb}^* V_{ud}\left\{\frac{\cos\theta_3}{\sqrt{3}}[f_{B_c}(F_{fa;H}^{b_1^+ f_1^u}+F_{fa;H}^{f_1^d b_1^+})a_1\right.\\ &\quad +(M_{na;H}^{b_1^+ f_1^u}+M_{na;H}^{f_1^d b_1^+})C_1]+\frac{\sin\theta_3}{\sqrt{6}}[f_{B_c}\\ &\quad \left.\cdot(F_{fa;H}^{b_1^+ f_8^u}+F_{fa;H}^{f_8^d b_1^+})a_1+(M_{na;H}^{b_1^+ f_8^u}+M_{na;H}^{f_8^d b_1^+})C_1]\right\}\ , \end{aligned} \tag{85}$$

$$\begin{aligned}\mathcal{M}^H(B_c\to b_1^+ f'') &= V_{cb}^* V_{ud}\left\{\frac{-\sin\theta_3}{\sqrt{3}}[f_{B_c}(F_{fa;H}^{b_1^+ f_1^u}+F_{fa;H}^{f_1^d b_1^+})a_1\right.\\ &\quad +(M_{na;H}^{b_1^+ f_1^u}+M_{na;H}^{f_1^d b_1^+})C_1]+\frac{\cos\theta_3}{\sqrt{6}}[f_{B_c}\\ &\quad \left.\cdot(F_{fa;H}^{b_1^+ f_8^u}+F_{fa;H}^{f_8^d b_1^+})a_1+(M_{na;H}^{b_1^+ f_8^u}+M_{na;H}^{f_8^d b_1^+})C_1]\right\}\ , \end{aligned} \tag{86}$$

$$\begin{aligned}\mathcal{M}^H(B_c\to a_1^+ h') &= V_{cb}^* V_{ud}\left\{\frac{\cos\theta_1}{\sqrt{3}}[f_{B_c}(F_{fa;H}^{a_1^+ h_1^u}+F_{fa;H}^{h_1^d a_1^+})a_1\right.\\ &\quad +(M_{na;H}^{a_1^+ h_1^u}+M_{na;H}^{h_1^d a_1^+})C_1]+\frac{\sin\theta_1}{\sqrt{6}}[f_{B_c}\\ &\quad \left.\cdot(F_{fa;H}^{a_1^+ h_8^u}+F_{fa;H}^{h_8^d a_1^+})a_1+(M_{na;H}^{a_1^+ h_8^u}+M_{na;H}^{h_8^d a_1^+})C_1]\right\}\ , \end{aligned} \tag{87}$$

$$\begin{aligned}\mathcal{M}^H(B_c\to a_1^+ h'') &= V_{cb}^* V_{ud}\left\{\frac{-\sin\theta_1}{\sqrt{3}}[f_{B_c}(F_{fa;H}^{a_1^+ h_1^u}+F_{fa;H}^{h_1^d a_1^+})a_1\right.\\ &\quad +(M_{na;H}^{a_1^+ h_1^u}+M_{na;H}^{h_1^d a_1^+})C_1]+\frac{\cos\theta_1}{\sqrt{6}}[f_{B_c}\\ &\quad \left.\cdot(F_{fa;H}^{a_1^+ h_8^u}+F_{fa;H}^{h_8^d a_1^+})a_1+(M_{na;H}^{a_1^+ h_8^u}+M_{na;H}^{h_8^d a_1^+})C_1]\right\}\ , \end{aligned} \tag{88}$$

$$\begin{aligned}\mathcal{M}^H(B_c\to b_1^+ h') &= V_{cb}^* V_{ud}\left\{\frac{\cos\theta_1}{\sqrt{3}}[f_{B_c}(F_{fa;H}^{b_1^+ h_1^u}+F_{fa;H}^{h_1^d b_1^+})a_1\right.\\ &\quad +(M_{na;H}^{b_1^+ h_1^u}+M_{na;H}^{h_1^d b_1^+})C_1]+\frac{\sin\theta_1}{\sqrt{6}}[f_{B_c}\\ &\quad \left.\cdot(F_{fa;H}^{b_1^+ h_8^u}+F_{fa;H}^{h_8^d b_1^+})a_1+(M_{na;H}^{b_1^+ h_8^u}+M_{na;H}^{h_8^d b_1^+})C_1]\right\}\ , \end{aligned} \tag{89}$$

$$\begin{aligned}\mathcal{M}^H(B_c\to b_1^+ h'') &= V_{cb}^* V_{ud}\left\{\frac{-\sin\theta_1}{\sqrt{3}}[f_{B_c}(F_{fa;H}^{b_1^+ h_1^u}+F_{fa;H}^{h_1^d b_1^+})a_1\right.\\ &\quad +(M_{na;H}^{b_1^+ h_1^u}+M_{na;H}^{h_1^d b_1^+})C_1]+\frac{\cos\theta_1}{\sqrt{6}}[f_{B_c}\\ &\quad \left.\cdot(F_{fa;H}^{b_1^+ h_8^u}+F_{fa;H}^{h_8^d b_1^+})a_1+(M_{na;H}^{b_1^+ h_8^u}+M_{na;H}^{h_8^d b_1^+})C_1]\right\}\ , \end{aligned} \tag{90}$$

$$\begin{aligned}\mathcal{M}^H(B_c \to \overline{K'}^0 K'^+) \;=\; V_{cb}^* V_{ud} \Big\{ & -\sin^2\theta_K (f_{B_c} F_{fa;H}^{\overline{K_{1A}}^0 K_{1A}} a_1 + M_{na;H}^{\overline{K_{1A}}^0 K_{1A}} C_1) \\ & -\cos\theta_K \sin\theta_K (f_{B_c} F_{fa;H}^{\overline{K_{1A}}^0 K_{1B}} a_1 + M_{na;H}^{\overline{K_{1A}}^0 K_{1B}} C_1) \\ & +\cos\theta_K \sin\theta_K (f_{B_c} F_{fa;H}^{\overline{K_{1B}}^0 K_{1A}} a_1 + M_{na;H}^{\overline{K_{1B}}^0 K_{1A}} C_1) \\ & +\cos^2\theta_K (f_{B_c} F_{fa;H}^{\overline{K_{1B}}^0 K_{1B}} a_1 + M_{na;H}^{\overline{K_{1B}}^0 K_{1B}} C_1) \Big\} \;, \end{aligned} \tag{91}$$

$$\begin{aligned}\mathcal{M}^H(B_c \to \overline{K'}^0 K''^+) \;=\; V_{cb}^* V_{ud} \Big\{ & -\cos\theta_K \sin\theta_K (f_{B_c} F_{fa;H}^{\overline{K_{1A}}^0 K_{1A}} a_1 + M_{na;H}^{\overline{K_{1A}}^0 K_{1A}} C_1) \\ & +\sin^2\theta_K (f_{B_c} F_{fa;H}^{\overline{K_{1A}}^0 K_{1B}} a_1 + M_{na;H}^{\overline{K_{1A}}^0 K_{1B}} C_1) \\ & +\cos^2\theta_K (f_{B_c} F_{fa;H}^{\overline{K_{1B}}^0 K_{1A}} a_1 + M_{na;H}^{\overline{K_{1B}}^0 K_{1A}} C_1) \\ & -\cos\theta_K \sin\theta_K (f_{B_c} F_{fa;H}^{\overline{K_{1B}}^0 K_{1B}} a_1 + M_{na;H}^{\overline{K_{1B}}^0 K_{1B}} C_1) \Big\} \;, \end{aligned} \tag{92}$$

$$\begin{aligned}\mathcal{M}^H(B_c \to \overline{K''}^0 K'^+) \;=\; V_{cb}^* V_{ud} \Big\{ & \cos\theta_K \sin\theta_K (f_{B_c} F_{fa;H}^{\overline{K_{1A}}^0 K_{1A}} a_1 + M_{na;H}^{\overline{K_{1A}}^0 K_{1A}} C_1) \\ & +\cos^2\theta_K (f_{B_c} F_{fa;H}^{\overline{K_{1A}}^0 K_{1B}} a_1 + M_{na;H}^{\overline{K_{1A}}^0 K_{1B}} C_1) \\ & +\sin^2\theta_K (f_{B_c} F_{fa;H}^{\overline{K_{1B}}^0 K_{1A}} a_1 + M_{na;H}^{\overline{K_{1B}}^0 K_{1A}} C_1) \\ & +\cos\theta_K \sin\theta_K (f_{B_c} F_{fa;H}^{\overline{K_{1B}}^0 K_{1B}} a_1 + M_{na;H}^{\overline{K_{1B}}^0 K_{1B}} C_1) \Big\} \;, \end{aligned} \tag{93}$$

$$\begin{aligned}\mathcal{M}^H(B_c \to \overline{K''}^0 K''^+) \;=\; V_{cb}^* V_{ud} \Big\{ & \cos^2\theta_K (f_{B_c} F_{fa;H}^{\overline{K_{1A}}^0 K_{1A}} a_1 + M_{na;H}^{\overline{K_{1A}}^0 K_{1A}} C_1) \\ & -\cos\theta_K \sin\theta_K (f_{B_c} F_{fa;H}^{\overline{K_{1A}}^0 K_{1B}} a_1 + M_{na;H}^{\overline{K_{1A}}^0 K_{1B}} C_1) \\ & +\cos\theta_K \sin\theta_K (f_{B_c} F_{fa;H}^{\overline{K_{1B}}^0 K_{1A}} a_1 + M_{na;H}^{\overline{K_{1B}}^0 K_{1A}} C_1) \\ & -\sin^2\theta_K (f_{B_c} F_{fa;H}^{\overline{K_{1B}}^0 K_{1B}} a_1 + M_{na;H}^{\overline{K_{1B}}^0 K_{1B}} C_1) \Big\} \;. \end{aligned} \tag{94}$$

(ii) For $\Delta S = 1$ processes,

$$\begin{aligned}\mathcal{M}^H(B_c \to K'^0 a_1^+) \;&=\; \sqrt{2}\mathcal{M}^H(B_c \to K'^+ a_1^0) \\ &=\; V_{cb}^* V_{us} \Big\{ \sin\theta_K [f_{B_c} F_{fa;H}^{K_{1A}^0 a_1^+} a_1 + M_{na;H}^{K_{1A}^0 a_1^+} C_1] \\ &\qquad + \cos\theta_K [f_{B_c} F_{fa;H}^{K_{1B}^0 a_1^+} a_1 + M_{na;H}^{K_{1B}^0 a_1^+} C_1] \Big\} \;, \end{aligned} \tag{95}$$

$$\begin{aligned}\mathcal{M}^H(B_c \to K''^0 a_1^+) \;&=\; \sqrt{2}\mathcal{M}^H(B_c \to K''^+ a_1^0) \\ &=\; V_{cb}^* V_{us} \Big\{ \cos\theta_K [f_{B_c} F_{fa;H}^{K_{1A}^0 a_1^+} a_1 + M_{na;H}^{K_{1A}^0 a_1^+} C_1] \\ &\qquad - \sin\theta_K [f_{B_c} F_{fa;H}^{K_{1B}^0 a_1^+} a_1 + M_{na;H}^{K_{1B}^0 a_1^+} C_1] \Big\} \;, \end{aligned} \tag{96}$$

$$\begin{aligned}\mathcal{M}^H(B_c\to K'^0 b_1^+) &= \sqrt{2}\mathcal{M}^H(B_c\to K'^+ b_1^0)\\ &= V_{cb}^*V_{us}\Big\{\sin\theta_K[f_{B_c}F_{fa;H}^{K_{1A}^0 b_1^+}a_1+M_{na;H}^{K_{1A}^0 b_1^+}C_1]\\ &\quad+\cos\theta_K[f_{B_c}F_{fa;H}^{K_{1B}^0 b_1^+}a_1+M_{na;H}^{K_{1B}^0 b_1^+}C_1]\Big\}\ ,\end{aligned}\tag{97}$$

$$\begin{aligned}\mathcal{M}^H(B_c\to K''^0 b_1^+) &= \sqrt{2}\mathcal{M}^H(B_c\to K''^+ b_1^0)\\ &= V_{cb}^*V_{us}\Big\{\cos\theta_K[f_{B_c}F_{fa;H}^{K_{1A}^0 b_1^+}a_1+M_{na;H}^{K_{1A}^0 b_1^+}C_1]\\ &\quad-\sin\theta_K[f_{B_c}F_{fa;H}^{K_{1B}^0 b_1^+}a_1+M_{na;H}^{K_{1B}^0 b_1^+}C_1]\Big\}\ ,\end{aligned}\tag{98}$$

$$\begin{aligned}\mathcal{M}^H(B_c\to K'^+ f') &= V_{cb}^*V_{us}\Big\{\frac{\cos\theta_3\sin\theta_K}{\sqrt{3}}[f_{B_c}(F_{fa;H}^{K_{1A}f_1^u}+F_{fa;H}^{f_1^s K_{1A}})a_1\\ &\quad+(M_{na;H}^{K_{1A}f_1^u}+M_{na;H}^{f_1^s K_{1A}})C_1]+\frac{\sin\theta_3\sin\theta_K}{\sqrt{6}}[f_{B_c}\\ &\quad\cdot(F_{fa;H}^{K_{1A}f_8^u}-2F_{fa;H}^{f_8^s K_{1A}})a_1+(M_{na;H}^{K_{1A}f_8^u}-2M_{na;H}^{f_8^s K_{1A}})\\ &\quad\cdot C_1]+\frac{\cos\theta_3\cos\theta_K}{\sqrt{3}}[f_{B_c}(F_{fa;H}^{K_{1B}f_1^u}+F_{fa;H}^{f_1^s K_{1B}})a_1\\ &\quad+(M_{na;H}^{K_{1B}f_1^u}+M_{na;H}^{f_1^s K_{1B}})C_1+\frac{\cos\theta_K\sin\theta_3}{\sqrt{6}}[f_{B_c}\\ &\quad\cdot(F_{fa;H}^{K_{1B}f_8^u}-2F_{fa;H}^{f_8^s K_{1B}})a_1+(M_{na;H}^{K_{1B}f_8^u}-2M_{na;H}^{f_8^s K_{1B}})C_1]\Big\}\ ,\end{aligned}\tag{99}$$

$$\begin{aligned}\mathcal{M}^H(B_c\to K'^+ f'') &= V_{cb}^*V_{us}\Big\{\frac{-\sin\theta_3\sin\theta_K}{\sqrt{3}}[f_{B_c}(F_{fa;H}^{K_{1A}f_1^u}+F_{fa;H}^{f_1^s K_{1A}})a_1\\ &\quad+(M_{na;H}^{K_{1A}f_1^u}+M_{na;H}^{f_1^s K_{1A}})C_1]+\frac{\cos\theta_3\sin\theta_K}{\sqrt{6}}[f_{B_c}\\ &\quad\cdot(F_{fa;H}^{K_{1A}f_8^u}-2F_{fa;H}^{f_8^s K_{1A}})a_1+(M_{na;H}^{K_{1A}f_8^u}-2M_{na;H}^{f_8^s K_{1A}})\\ &\quad\cdot C_1]-\frac{\cos\theta_K\sin\theta_3}{\sqrt{3}}[f_{B_c}(F_{fa;H}^{K_{1B}f_1^u}+F_{fa;H}^{f_1^s K_{1B}})a_1\\ &\quad+(M_{na;H}^{K_{1B}f_1^u}+M_{na;H}^{f_1^s K_{1B}})C_1]+\frac{\cos\theta_K\cos\theta_3}{\sqrt{6}}[f_{B_c}\\ &\quad\cdot(F_{fa;H}^{K_{1B}f_8^u}-2F_{fa;H}^{f_8^s K_{1B}})a_1+(M_{na;H}^{K_{1B}f_8^u}-2M_{na;H}^{f_8^s K_{1B}})C_1]\Big\}\ ,\end{aligned}\tag{100}$$

$$
\begin{aligned}
\mathcal{M}^H(B_c\to K''^+f') \;=\; & V_{cb}^*V_{us}\left\{\frac{\cos\theta_3\cos\theta_K}{\sqrt{3}}[f_{B_c}(F_{fa;H}^{K_{1A}f_1^u}+F_{fa;H}^{f_1^sK_{1A}})a_1\right.\\
&+(M_{na;H}^{K_{1A}f_1^u}+M_{na;H}^{f_1^sK_{1A}})C_1]+\frac{\cos\theta_K\sin\theta_3}{\sqrt{6}}[f_{B_c}\\
&\cdot(F_{fa;H}^{K_{1A}f_8^u}-2F_{fa;H}^{f_8^sK_{1A}})a_1+(M_{na;H}^{K_{1A}f_8^u}-2M_{na;H}^{f_8^sK_{1A}})\\
&\cdot C_1]-\frac{\cos\theta_3\sin\theta_K}{\sqrt{3}}[f_{B_c}(F_{fa;H}^{K_{1B}f_1^u}+F_{fa;H}^{f_1^sK_{1B}})a_1\\
&+(M_{na;H}^{K_{1B}f_1^u}+M_{na;H}^{f_1^sK_{1B}})C_1]-\frac{\sin\theta_K\sin\theta_3}{\sqrt{6}}[f_{B_c}\\
&\left.\cdot(F_{fa;H}^{K_{1B}f_8^u}-2F_{fa;H}^{f_8^sK_{1B}})a_1+(M_{na;H}^{K_{1B}f_8^u}-2M_{na;H}^{f_8^sK_{1B}})C_1]\right\} \;, \qquad (101)
\end{aligned}
$$

$$
\begin{aligned}
\mathcal{M}^H(B_c\to K''^+f'') \;=\; & V_{cb}^*V_{us}\left\{\frac{-\cos\theta_K\sin\theta_3}{\sqrt{3}}[f_{B_c}(F_{fa;H}^{K_{1A}f_1^u}+F_{fa;H}^{f_1^sK_{1A}})a_1\right.\\
&+(M_{na;H}^{K_{1A}f_1^u}+M_{na;H}^{f_1^sK_{1A}})C_1]+\frac{\cos\theta_3\cos\theta_K}{\sqrt{6}}[f_{B_c}\\
&\cdot(F_{fa;H}^{K_{1A}f_8^u}-2F_{fa;H}^{f_8^sK_{1A}})a_1+(M_{na;H}^{K_{1A}f_8^u}-2M_{na;H}^{f_8^sK_{1A}})\\
&\cdot C_1]+\frac{\sin\theta_3\sin\theta_K}{\sqrt{3}}[f_{B_c}(F_{fa;H}^{K_{1B}f_1^u}+F_{fa;H}^{f_1^sK_{1B}})a_1\\
&+(M_{na;H}^{K_{1B}f_1^u}+M_{na;H}^{f_1^sK_{1B}})C_1]-\frac{\cos\theta_3\sin\theta_K}{\sqrt{6}}[f_{B_c}\\
&\left.\cdot(F_{fa;H}^{K_{1B}f_8^u}-2F_{fa;H}^{f_8^sK_{1B}})a_1+(M_{na;H}^{K_{1B}f_8^u}-2M_{na;H}^{f_8^sK_{1B}})C_1]\right\} \;, \qquad (102)
\end{aligned}
$$

$$
\begin{aligned}
\mathcal{M}^H(B_c\to K'^+h') \;=\; & V_{cb}^*V_{us}\left\{\frac{\cos\theta_3\sin\theta_K}{\sqrt{3}}[f_{B_c}(F_{fa;H}^{K_{1A}h_1^u}+F_{fa;H}^{h_1^sK_{1A}})a_1\right.\\
&+(M_{na;H}^{K_{1A}h_1^u}+M_{na;H}^{h_1^sK_{1A}})C_1]+\frac{\sin\theta_3\sin\theta_K}{\sqrt{6}}[f_{B_c}\\
&\cdot(F_{fa;H}^{K_{1A}h_8^u}-2F_{fa;H}^{h_8^sK_{1A}})a_1+(M_{na;H}^{K_{1A}h_8^u}-2M_{na;H}^{h_8^sK_{1A}})\\
&\cdot C_1]+\frac{\cos\theta_3\cos\theta_K}{\sqrt{3}}[f_{B_c}(F_{fa;H}^{K_{1B}h_1^u}+F_{fa;H}^{h_1^sK_{1B}})a_1\\
&+(M_{na;H}^{K_{1B}h_1^u}+M_{na;H}^{h_1^sK_{1B}})C_1]+\frac{\cos\theta_K\sin\theta_3}{\sqrt{6}}[f_{B_c}\\
&\left.\cdot(F_{fa;H}^{K_{1B}h_8^u}-2F_{fa;H}^{h_8^sK_{1B}})a_1+(M_{na;H}^{K_{1b}h_8^u}-2M_{na;H}^{h_8^sK_{1B}})C_1]\right\} \;, \qquad (103)
\end{aligned}
$$

$$\mathcal{M}^H(B_c \to K'^+h'') = V_{cb}^*V_{us}\left\{\frac{-\sin\theta_3\sin\theta_K}{\sqrt{3}}[f_{B_c}(F_{fa;H}^{K_{1A}h_1^u} + F_{fa;H}^{h_1^sK_{1A}})a_1 + (M_{na;H}^{K_{1A}h_1^u} + M_{na;H}^{h_1^sK_{1A}})C_1] + \frac{\cos\theta_3\sin\theta_K}{\sqrt{6}}[f_{B_c} \cdot(F_{fa;H}^{K_{1A}h_8^u} - 2F_{fa;H}^{h_8^sK_{1A}})a_1 + (M_{na;H}^{K_{1A}h_8^u} - 2M_{na;H}^{h_8^sK_{1A}}) \cdot C_1] - \frac{\cos\theta_K\sin\theta_3}{\sqrt{3}}[f_{B_c}(F_{fa;H}^{K_{1B}h_1^u} + F_{fa;H}^{h_1^sK_{1B}})a_1 + (M_{na;H}^{K_{1B}h_1^u} + M_{na;H}^{h_1^sK_{1B}})C_1] + \frac{\cos\theta_K\cos\theta_3}{\sqrt{6}}[f_{B_c} \cdot(F_{fa;H}^{K_{1B}h_8^u} - 2F_{fa;H}^{h_8^sK_{1B}})a_1 + (M_{na;H}^{K_{1b}h_8^u} - 2M_{na;H}^{h_8^sK_{1B}})C_1]\right\}, \quad (104)$$

$$\mathcal{M}^H(B_c \to K''^+h') = V_{cb}^*V_{us}\left\{\frac{\cos\theta_3\cos\theta_K}{\sqrt{3}}[f_{B_c}(F_{fa;H}^{K_{1A}h_1^u} + F_{fa;H}^{h_1^sK_{1A}})a_1 + (M_{na;H}^{K_{1A}h_1^u} + M_{na;H}^{h_1^sK_{1A}})C_1] + \frac{\cos\theta_K\sin\theta_3}{\sqrt{6}}[f_{B_c} \cdot(F_{fa;H}^{K_{1A}h_8^u} - 2F_{fa;H}^{h_8^sK_{1A}})a_1 + (M_{na;H}^{K_{1A}h_8^u} - 2M_{na;H}^{h_8^sK_{1A}}) \cdot C_1] - \frac{\cos\theta_3\sin\theta_K}{\sqrt{3}}[f_{B_c}(F_{fa;H}^{K_{1B}h_1^u} + F_{fa;H}^{h_1^sK_{1B}})a_1 + (M_{na;H}^{K_{1B}h_1^u} + M_{na;H}^{h_1^sK_{1B}})C_1] - \frac{\sin\theta_K\sin\theta_3}{\sqrt{6}}[f_{B_c} \cdot(F_{fa;H}^{K_{1B}h_8^u} - 2F_{fa;H}^{h_8^sK_{1B}})a_1 + (M_{na;H}^{K_{1b}h_8^u} - 2M_{na;H}^{h_8^sK_{1B}})C_1]\right\}, \quad (105)$$

$$\mathcal{M}^H(B_c \to K''^+h'') = V_{cb}^*V_{us}\left\{\frac{-\cos\theta_K\sin\theta_3}{\sqrt{3}}[f_{B_c}(F_{fa;H}^{K_{1A}h_1^u} + F_{fa;H}^{h_1^sK_{1A}})a_1 + (M_{na;H}^{K_{1A}h_1^u} + M_{na;H}^{h_1^sK_{1A}})C_1] + \frac{\cos\theta_3\cos\theta_K}{\sqrt{6}}[f_{B_c} \cdot(F_{fa;H}^{K_{1A}h_8^u} - 2F_{fa;H}^{h_8^sK_{1A}})a_1 + (M_{na;H}^{K_{1A}h_8^u} - 2M_{na;H}^{h_8^sK_{1A}}) \cdot C_1] + \frac{\sin\theta_3\sin\theta_K}{\sqrt{3}}[f_{B_c}(F_{fa;H}^{K_{1B}h_1^u} + F_{fa;H}^{h_1^sK_{1B}})a_1 + (M_{na;H}^{K_{1B}h_1^u} + M_{na;H}^{h_1^sK_{1B}})C_1] - \frac{\cos\theta_3\sin\theta_K}{\sqrt{6}}[f_{B_c} \cdot(F_{fa;H}^{K_{1B}h_8^u} - 2F_{fa;H}^{h_8^sK_{1B}})a_1 + (M_{na;H}^{K_{1b}h_8^u} - 2M_{na;H}^{h_8^sK_{1B}})C_1]\right\}. \quad (106)$$

IV. NUMERICAL RESULTS AND DISCUSSIONS

In this section, we will calculate numerically the BRs and polarization fractions for those considered sixty two $B_c \to VA/AV, AA$ decay modes. First of all, the central values of the input parameters to be used are given in the following,

Masses (GeV):

$$\begin{aligned}
m_W &= 80.41; \quad m_{B_c} = 6.286; \quad m_b = 4.8; \quad m_c = 1.5; \\
m_\phi &= 1.02; \quad m_{K^*} = 0.892; \quad m_\rho = 0.770; \quad m_\omega = 0.782; \\
m_{a_1} &= 1.23; \quad m_{K_{1A}} = 1.32; \quad m_{f_1} = 1.28; \quad m_{f_8} = 1.28; \\
m_{b_1} &= 1.21; \quad m_{K_{1B}} = 1.34; \quad m_{h_1} = 1.23; \quad m_{h_8} = 1.37; \qquad (107)
\end{aligned}$$

Decay constants (GeV):

$$\begin{aligned}
f_\phi &= 0.231; \quad f_\phi^T = 0.200; \quad f_{K^*} = 0.217; \quad f_{K^*}^T = 0.185; \\
f_\rho &= 0.209; \quad f_\rho^T = 0.165; \quad f_\omega = 0.195; \quad f_\omega^T = 0.145; \\
f_{a_1} &= 0.238; \quad f_{K_{1A}} = 0.250; \quad f_{f_1} = 0.245; \quad f_{f_8} = 0.239; \\
f_{b_1} &= 0.180; \quad f_{K_{1B}} = 0.190; \quad f_{h_1} = 0.180; \quad f_{h_8} = 0.190; \\
f_{B_c} &= 0.489; \qquad (108)
\end{aligned}$$

QCD scale and B_c meson lifetime:

$$\Lambda_{\overline{\mathrm{MS}}}^{(f=4)} = 0.250 \text{ GeV}, \quad \tau_{B_c^+} = 0.46 \text{ ps}. \qquad (109)$$

For the CKM matrix elements, here we adopt the Wolfenstein parametrization for the CKM matrix, and take $A = 0.814$ and $\lambda = 0.2257$, $\bar{\rho} = 0.135$ and $\bar{\eta} = 0.349$ [25]. In numerical calculations, central values of input parameters will be used implicitly unless otherwise stated.

For these considered $B_c \to M_2 M_3$ decays, the decay rate can be written explicitly as,

$$\Gamma = \frac{G_F^2 |\mathbf{P_c}|}{16\pi m_{B_c}^2} \sum_{\sigma=L,T} \mathcal{M}^{(\sigma)\dagger} \mathcal{M}^{(\sigma)} \qquad (110)$$

where $|\mathbf{P_c}| \equiv |\mathbf{P_{2z}}| = |\mathbf{P_{3z}}|$ is the momentum of either of the outgoing vector or axial-vector mesons.

Based on the helicity amplitudes (33), we can define the transversity amplitudes,

$$\mathcal{A}_L = -\xi m_{B_c}^2 \mathcal{M}_L, \quad \mathcal{A}_\parallel = \xi \sqrt{2} m_{B_c}^2 \mathcal{M}_N, \quad \mathcal{A}_\perp = \xi m_{B_c}^2 \sqrt{2(r^2-1)} \mathcal{M}_T \,. \qquad (111)$$

for the longitudinal, parallel, and perpendicular polarizations, respectively, with the normalization factor $\xi = \sqrt{G_F^2 \mathbf{P_c}/(16\pi m_{B_c}^2 \Gamma)}$ and the ratio $r = P_2 \cdot P_3/(m_2\, m_3)$. These amplitudes satisfy the relation,

$$|\mathcal{A}_L|^2 + |\mathcal{A}_\parallel|^2 + |\mathcal{A}_\perp|^2 = 1 \qquad (112)$$

following the summation in Eq. (110).

The polarization fractions $f_L, f_{||}$ and $f_\perp$ can be defined as,

$$f_{L(||,\perp)} = \frac{|\mathcal{A}_{L(||,\perp)}|^2}{|\mathcal{A}_L|^2 + |\mathcal{A}_{||}|^2 + |\mathcal{A}_\perp|^2}, \qquad (113)$$

With the analytic formulas for the complete decay amplitudes as given explicitly in Eqs. (53-106), by employing the input parameters and Eq.(110), we calculate and then present the pQCD predictions for the *CP*-averaged BRs and longitudinal polarization fractions (LPFs) of the considered decays with errors in Tables I-X. The dominant errors come from the uncertainties of charm quark mass $m_c = 1.5 \pm 0.15$ GeV and the combined Gegenbauer moments a_i of the relevant meson distribution amplitudes, respectively.

Based on the numerical results as given in Tables I-X, some remarks are in order:

- Among the considered sixty two pure annihilation $B_c \to AV/VA, AA$ decays, the pQCD predictions for the CP-averaged BRs of those $\Delta S = 0$ processes are generally much larger than those of $\Delta S = 1$ channels (one of the two final state mesons is a strange meson), the main reason is the enhancement of the large CKM factor $|V_{ud}/V_{us}|^2 \sim 19$ for those $\Delta S = 0$ decays as expected in general. Maybe there exists no such large differences for certain decays, which is just because the enhancement arising from the CKM factor is partially cancelled by the difference between the magnitude of individual decay amplitude.

- There is no CP violation for all these sixty two decays within the SM, since there is only one kind of tree operator involved in the decay amplitude of all considered B_c decays, which can be seen directly from Eq. (52).

- For the ten $B_c \to (a_1, b_1)V$ decays, the pQCD predictions of the BRs and LPFs for both $\Delta S = 0$ and $\Delta S = 1$ processes are listed in the Table I. As argued in Ref. [4], the LHCb experiments could observe the BRs of annihilation B_c meson decays at the level of 10^{-6}, the decays $B_c \to a_1\omega, b_1\rho$ will thus be detected at LHC because they are just within its reach. As for the polarization, all these ten decays are governed by the longitudinal contributions. The LPFs are around 95% within the theoretical errors except for $B_c \to a_1^+\omega, a_1 K^*$ modes ($\sim$ 85%), and for $B_c \to a_1\rho$ channels, $f_L(B_c \to a_1\rho) \sim 1$, which will be tested in the LHCb experiments.

- Since the behavior of b_1 meson is contrary to that of a_1 meson, one can find that $Br(B_c \to b_1\rho) > Br(B_c \to a_1\rho)$ as given in Table I and the ratio of the corresponding BRs for $B_c \to a_1\rho$ and $B_c \to b_1\rho$ is that

$$\frac{Br(B_c \to b_1^+\rho^0)}{Br(B_c \to a_1^+\rho^0)} = \frac{Br(B_c \to b_1^0\rho^+)}{Br(B_c \to a_1^0\rho^+)} \approx 13.2 \,, \tag{114}$$

Similarly, for $B_c \to a_1K^*, b_1K^*$ decays, the BRs of the latter modes are larger than that of the former ones and

$$\frac{Br(B_c \to b_1^+K^{*0})}{Br(B_c \to a_1^+K^{*0})} = \frac{Br(B_c \to b_1^0K^{*+})}{Br(B_c \to a_1^0K^{*+})} \approx 5.5 \,, \tag{115}$$

The above two ratios exhibit the annihilation decay pattern consistent with those as shown in Ref. [23].

TABLE I: The pQCD predictions of BRs and LPFs for $B_c \to (a_1, b_1)(\rho, K^*, \omega)$ decays. The source of the dominant errors is explained in the text.

$\Delta S = 0$			$\Delta S = 0$		
Decay modes	BRs (10^{-7})	LPFs (%)	Decay modes	BRs (10^{-6})	LPFs (%)
$\mathrm{B_c} \to \rho^+\mathrm{a}_1^0$	$7.5^{+0.1}_{-0.2}(m_c)^{+3.0}_{-2.8}(a_i)$	$99.2^{+0.3}_{-0.4}$	$\mathrm{B_c} \to \rho^+\mathrm{b}_1^0$	$9.9^{+4.7}_{-3.9}(m_c)^{+5.6}_{-4.4}(a_i)$	$93.8^{+2.5}_{-4.4}$
$\mathrm{B_c} \to \mathrm{a}_1^+\rho^0$	$7.5^{+0.1}_{-0.2}(m_c)^{+3.0}_{-2.8}(a_i)$	$99.2^{+0.3}_{-0.4}$	$\mathrm{B_c} \to \mathrm{b}_1^+\rho^0$	$9.9^{+4.5}_{-4.0}(m_c)^{+5.7}_{-4.2}(a_i)$	$93.8^{+2.5}_{-4.4}$
$\mathrm{B_c} \to \mathrm{a}_1^+\omega$	$20.2^{+3.0}_{-0.0}(m_c)^{+7.8}_{-4.8}(a_i)$	$84.7^{+5.0}_{-4.4}$	$\mathrm{B_c} \to \mathrm{b}_1^+\omega$	$0.6^{+0.5}_{-0.4}(m_c)^{+0.3}_{-0.4}(a_i)$	$96.3^{+2.3}_{-7.5}$
$\Delta S = 1$			$\Delta S = 1$		
Decay modes	BRs (10^{-8})	LPFs (%)	Decay modes	BRs (10^{-7})	LPFs (%)
$\mathrm{B_c} \to \mathrm{a}_1^+\mathrm{K}^{*0}$	$6.5^{+0.2}_{-0.0}(m_c)^{+3.5}_{-2.5}(a_i)$	$83.6^{+5.3}_{-7.5}$	$\mathrm{B_c} \to \mathrm{b}_1^+\mathrm{K}^{*0}$	$3.6^{+1.1}_{-0.8}(m_c)^{+1.8}_{-1.6}(a_i)$	$91.2^{+2.5}_{-4.1}$
$\mathrm{B_c} \to \mathrm{K}^{*+}\mathrm{a}_1^0$	$3.3^{+0.1}_{-0.0}(m_c)^{+1.7}_{-1.3}(a_i)$	$83.6^{+5.3}_{-7.5}$	$\mathrm{B_c} \to \mathrm{K}^{*+}\mathrm{b}_1^0$	$1.8^{+0.5}_{-0.4}(m_c)^{+0.9}_{-0.7}(a_i)$	$91.2^{+2.5}_{-4.1}$

TABLE II: Same as Table I but for $B_c \to (a_1, b_1)(a_1, b_1)$ decays.

$\Delta S = 0$ Decay modes	BRs (10^{-5})	LPFs (%)	$\Delta S = 0$ Decay modes	BRs (10^{-5})	LPFs (%)
$\mathrm{B_c \to a_1^+ a_1^0}$	0.0	–	$\mathrm{B_c \to b_1^+ b_1^0}$	0.0	–
$\mathrm{B_c \to a_1^+ b_1^0}$	$2.2^{+0.6}_{-0.5}(m_c)^{+1.1}_{-0.9}(a_i)$	$92.4^{+1.9}_{-2.8}$	$\mathrm{B_c \to b_1^+ a_1^0}$	$2.2^{+0.6}_{-0.5}(m_c)^{+1.1}_{-0.8}(a_i)$	$91.8^{+2.0}_{-2.6}$

- Analogous to $B_c \to \rho^+\rho^0$ decay [2], the contributions from $\bar{u}u$ and $\bar{d}d$ components cancel each other exactly and result in the zero BRs for $B_c \to a_1^+ a_1^0$ and $B_c \to b_1^+ b_1^0$. Any other nonzero data for these two channels may indicate the effects of exotic new physics. While for $B_c \to a_1^+ b_1^0$ and $B_c \to b_1^+ a_1^0$, as expected from the analytic expressions, Eqs. (81,82), due to the same component of $u\bar{u} - d\bar{d}$ involved in both axial-vector a_1^0 and b_1^0 mesons at the quark level, the pQCD predictions for the BRs and LPFs as given in Table II show the identical results as they should be,

$$\begin{aligned} Br(B_c \to a_1^+ b_1^0) &= Br(B_c \to b_1^+ a_1^0) \approx 2.2 \times 10^{-5} , \\ f_L(B_c \to a_1^+ b_1^0) &= f_L(B_c \to b_1^+ a_1^0) \approx 92\% . \end{aligned} \tag{116}$$

  where the large BRs ($\sim 10^{-5}$) are within the reach of the LHCb experiments [4] and could be detected at LHC.

- Since the $^3P_1$ meson behaves like the vector meson and $f_{a_1} \sim f_\rho$ from Eq. (108), the pQCD predictions of BRs exhibit the good consistency generally for $B_c \to a_1^+\omega$ and $B_c \to \rho^+\omega$, $B_c \to a_1^+ K^{*0}$ and $B_c \to \rho^+ K^{*0}$, $B_c \to a_1^+ b_1^0(a_1^0 b_1^+)$ and $B_c \to \rho^+ b_1^0(\rho^0 b_1^+)$ decays, respectively, within the theoretical errors as roughly estimated. As for the polarizations, which can well manifest the helicity structure for the corresponding modes, the LPFs present the different features from the decay rates except for $B_c \to a_1^+ b_1^0(a_1^0 b_1^+)$ and $B_c \to \rho^+ b_1^0(\rho^0 b_1^+)$ decays. From Table I, the LPFs for $B_c \to a_1^+\omega$ and $B_c \to a_1^+ K^{*0}$ can be read straight forward as: $f_L(B_c \to a_1^+\omega) = (84.7^{+5.0}_{-4.4})\%$ and $f_L(B_c \to a_1^+ K^{*0}) = (83.6^{+5.3}_{-7.5})\%$. As given in Ref. [2], $f_L(B_c \to \rho^+\omega) = (92.9^{+2.0}_{-0.1})\%$ and $f_L(B_c \to \rho^+ K^{*0}) = (94.9^{+2.0}_{-1.4})\%$, where the various errors as specified have been added in quadrature. The above results and discussions would be tested with high precision by the relevant experiments operated

TABLE III: Same as Table I but for $B_c \to (\rho, K^*)(f_1(1285), f_1(1420))$ decays.

$\Delta S = 0$	$\theta_3 = 38^\circ$		$\theta_3 = 50^\circ$	
Decay modes	BRs (10^{-6})	LPFs (%)	BRs(10^{-6})	LPFs (%)
$\mathrm{B_c \to \rho^+ f_1(1285)}$	$2.1^{+0.3}_{-0.0}(m_c)^{+0.8}_{-0.4}(a_i)$	$82.6^{+5.4}_{-3.8}$	$1.9^{+0.3}_{-0.0}(m_c)^{+0.7}_{-0.3}(a_i)$	$82.3^{+5.6}_{-3.8}$
$\mathrm{B_c \to \rho^+ f_1(1420)} \times 10^a$	$0.4^{+0.0}_{-0.1}(m_c)^{+0.8}_{-0.2}(a_i)$	$88.7^{+11.6}_{-9.2}$	$2.2^{+0.2}_{-0.0}(m_c)^{+2.2}_{-0.8}(a_i)$	$85.7^{+8.6}_{-6.9}$
$\Delta S = 1$	$\theta_3 = 38^\circ$		$\theta_3 = 50^\circ$	
Decay modes	BRs (10^{-7})	LPFs (%)	BRs (10^{-7})	LPFs (%)
$\mathrm{B_c \to K^{*+} f_1(1285)} \times 10$	$1.6^{+0.3}_{-0.0}(m_c)^{+1.5}_{-0.6}(a_i)$	$61.0^{+24.2}_{-22.2}$	$0.4^{+0.1}_{-0.0}(m_c)^{+0.5}_{-0.2}(a_i)$	$33.7^{+56.0}_{-38.6}$
$\mathrm{B_c \to K^{*+} f_1(1420)}$	$1.1^{+0.1}_{-0.0}(m_c)^{+0.4}_{-0.4}(a_i)$	$85.4^{+4.5}_{-5.8}$	$1.2^{+0.2}_{-0.0}(m_c)^{+0.5}_{-0.3}(a_i)$	$83.9^{+5.2}_{-6.3}$

[a] Here, the factor 10 is specifically used for the BRs. The following ones have the same meaning.

at the ongoing LHC and forthcoming Super-B to identify the helicity structure even decay mechanism in these considered channels.

- In Table III, from the pQCD predictions of the BRs and LPFs for $B_c \to \rho^+(f_1(1285), f_1(1420))(\Delta S = 0)$ and $B_c \to K^{*+}(f_1(1285), f_1(1420))(\Delta S = 1)$ decays, one can observe that the BRs of $B_c \to \rho^+ f_1(1420), K^{*+} f_1(1285)$ are more sensitive than those of $B_c \to \rho^+ f_1(1285), K^{*+} f_1(1420)$ to the mixing angle θ_3,

$$\frac{Br(B_c \to \rho^+ f_1(1420))|_{\theta_3=50^\circ}}{Br(B_c \to \rho^+ f_1(1420))|_{\theta_3=38^\circ}} \approx 5.5 \; ; \tag{117}$$

$$\frac{Br(B_c \to K^{*+} f_1(1285))|_{\theta_3=38^\circ}}{Br(B_c \to K^{*+} f_1(1285))|_{\theta_3=50^\circ}} \approx 4.0 \; ; \tag{118}$$

These two relations, Eqs. (117,118), can be understood as that the interferences between $B_c \to \rho^+ f_1 (B_c \to K^{*+} f_1)$ and $B_c \to \rho^+ f_8 (B_c \to K^{*+} f_8)$ become highly constructive(destructive) to $B_c \to \rho^+ f_1(1420)(B_c \to K^{*+} f_1(1285))$ with the mixing angle θ_3 changing from 38° to 50°. Moreover,

$$\frac{Br(B_c \to \rho^+ f_1(1285))}{Br(B_c \to \rho^+ f_1(1420))} \approx \begin{cases} 52.5 & \text{for} \quad \theta_3 = 38^\circ \\ 8.6 & \text{for} \quad \theta_3 = 50^\circ \end{cases} \; ; \tag{119}$$

$$\frac{Br(B_c \to K^{*+} f_1(1420))}{Br(B_c \to K^{*+} f_1(1285))} \approx \begin{cases} 6.9 & \text{for} \quad \theta_3 = 38^\circ \\ 30.0 & \text{for} \quad \theta_3 = 50^\circ \end{cases} \; ; \tag{120}$$

From the decay amplitudes as given in Eqs. (59,60,73,74), the above two relations can be understood as follows: (a) for $B_c \to \rho^+(f_1(1285), f_1(1420))$ decays, the mixing coefficients for the former decay are $\cos\theta_3$ and $\sin\theta_3$, while that for the latter one are $-\sin\theta_3$ and $\cos\theta_3$. For the common component $q\bar{q}$, it is found that the contributions from $B_c \to \rho^+ f_1$ and $B_c \to \rho^+ f_8$ interfere constructively(destructively) for $B_c \to \rho^+ f_1(1285)(B_c \to \rho^+ f_1(1420))$; (b) for $B_c \to K^{*+}(f_1(1285), f_1(1420))$ channels, the mixing parameters remain unchanged, however, a new part of contribution from $s\bar{s}$ component involved in both f_1 and f_8 with different signs results in the construction(destruction) to $B_c \to K^{*+} f_1(1420)(B_c \to K^{*+} f_1(1285))$. Additionally, the LPFs for these decays are stable to the mixing angle and play the dominant role except for $f_L(B_c \to K^{*+} f_1(1285))$, whose value change from 61.0% at $\theta_3 = 38^\circ$ to 33.7% at $\theta_3 = 50^\circ$, which will be confronted with the relevant experiments in the future.

TABLE IV: Same as Table I but for $B_c \to (\rho, K^*)(h_1(1170), h_1(1380))$ decays.

$\Delta S = 0$	$\theta_1 = 10^\circ$		$\theta_1 = 45^\circ$	
Decay modes	BRs (10^{-7})	LPFs (%)	BRs (10^{-7})	LPFs (%)
$\mathrm{B_c} \to \rho^+ \mathrm{h_1}(1170)$	$6.4^{+4.6}_{-4.1}(m_c)^{+2.2}_{-3.9}(a_i)$	$96.4^{+1.7}_{-7.0}$	$8.6^{+7.4}_{-5.1}(m_c)^{+2.7}_{-3.4}(a_i)$	$96.3^{+1.7}_{-5.4}$
$\mathrm{B_c} \to \rho^+ \mathrm{h_1}(1380)$	$2.5^{+2.6}_{-0.8}(m_c)^{+2.0}_{-1.4}(a_i)$	$96.3^{+2.1}_{-2.6}$	$0.3^{+0.2}_{-0.2}(m_c)^{+0.6}_{-0.1}(a_i)$	$98.0^{+1.7}_{-2.8}$
$\Delta S = 1$	$\theta_1 = 10^\circ$		$\theta_1 = 45^\circ$	
Decay modes	BRs (10^{-7})	LPFs (%)	BRs (10^{-7})	LPFs (%)
$\mathrm{B_c} \to \mathrm{K}^{*+} \mathrm{h_1}(1170)$	$0.2^{+0.1}_{-0.1}(m_c)^{+0.0}_{-0.1}(a_i)$	$82.3^{+6.2}_{-9.5}$	$2.1^{+0.6}_{-0.6}(m_c)^{+1.1}_{-0.8}(a_i)$	$89.5^{+3.4}_{-5.1}$
$\mathrm{B_c} \to \mathrm{K}^{*+} \mathrm{h_1}(1380)$	$4.8^{+2.2}_{-1.9}(m_c)^{+2.4}_{-2.0}(a_i)$	$93.2^{+2.2}_{-4.5}$	$2.9^{+1.7}_{-1.3}(m_c)^{+1.4}_{-1.1}(a_i)$	$94.9^{+1.8}_{-4.1}$

- The pQCD predictions for $B_c \to (\rho^+, K^{*+})h_1$ decays, as given in Table IV, can be explained in a similar way as for $B_c \to (\rho^+, K^{*+})f_1$.

- The numerical pQCD results for $\Delta S = 0$ $B_c \to (a_1^+, b_1^+)(f_1(1285), f_1(1420))$ decays, as given in Table V, can be commented in order: (a) the BRs of these modes depend weakly on the mixing angle θ_3 except for $B_c \to a_1^+ f_1(1420)$; (b) these 4 considered decays are governed by the longitudinal contributions for both $\theta_3 = 38°$ and $\theta_3 = 50°$; (c) as mentioned in the text above, 1^3P_1 meson behaves close to the vector meson, the phenomenology of $B_c \to a_1^+(f_1(1285), f_1(1420))$ can therefore be understood as that of $B_c \to \rho^+(f_1(1285), f_1(1420))$; (d) the mixing factors $\cos\theta_3$ and $\sin\theta_3$ make the interference between $B_c \to (a_1^+, b_1^+)f_1$ and $B_c \to (a_1^+, b_1^+)f_8$ constructive (destructive) to $B_c \to (a_1^+, b_1^+)f_1(1285)(B_c \to (a_1^+, b_1^+)f_1(1420))$.

- From the predictions for $B_c \to (a_1^+, b_1^+)(h_1(1170), h_1(1380))$ presented in Table VI, some discussions could be addressed as: (a) since the behavior of 1^1P_1 meson is different even contrary to that of 1^3P_1 meson, a surprisingly large branching ratio for $B_c \to b_1^+ h_1(1700)(\sim 10^{-4})$ with the constructive effects induced by the interference between $B_c \to b_1^+ h_1$ and $B_c \to b_1^+ h_8$ is produced, which will be tested stringently by the forthcoming relevant LHC experiments; (b) once the large BRs are verified by the measurements, the mixing angle θ_1 could be well determined to improve the precision of the perturbative calculations; (c) except for $B_c \to b_1^+ h_1(1170)$ decay, the rest three channels are sensitive significantly to the mixing angle θ_1; (d) similar to $B_c \to (a_1^+, b_1^+)(f_1(1285), f_1(1420))$ decays, the longitudinal components play the dominant role for these 4 channels.

- For the $\Delta S = 0$ $B_c \to \overline{K^*}^0 K_1^+$ and $B_c \to \overline{K_1} K^{*+}$ decays, one can see from Table VII that the BRs are large in the range of $10^{-6} \sim 10^{-5}$, which can be detected at the ongoing LHC and forthcoming Super B experiments. Moreover, the corresponding ratios of the BRs for these considered channels

$$\frac{Br(B_c \to \overline{K^*}^0 K_1(1270)^+)}{Br(B_c \to \overline{K^*}^0 K_1(1400)^+)} = \frac{Br(B_c \to \overline{K_1}(1270)^0 K^{*+})}{Br(B_c \to \overline{K_1}(1400)^0 K^{*+})} \approx 1.7 , \tag{121}$$

for $\theta_K = 45°$, while

$$\frac{Br(B_c \to \overline{K^*}^0 K_1(1270)^+)}{Br(B_c \to \overline{K^*}^0 K_1(1400)^+)} = \frac{Br(B_c \to \overline{K_1}(1270)^0 K^{*+})}{Br(B_c \to \overline{K_1}(1400)^0 K^{*+})} \approx \frac{1}{1.7} , \tag{122}$$

TABLE V: Same as Table I but for $B_c \to (a_1^+, b_1^+)(f_1(1285), f_1(1420))$ decays.

$\Delta S = 0$	$\theta_3 = 38°$		$\theta_3 = 50°$	
Decay modes	BRs (10^{-6})	LPFs (%)	BRs (10^{-6})	LPFs (%)
$B_c \to a_1(1260)^+ f_1(1285)$	$6.5^{+1.0}_{-0.9}(m_c)^{+0.5}_{-1.0}(a_i)$	$83.6^{+2.4}_{-4.1}$	$6.1^{+1.0}_{-0.9}(m_c)^{+0.4}_{-0.9}(a_i)$	$84.0^{+2.3}_{-4.0}$
$B_c \to a_1(1260)^+ f_1(1420) \times 10$	$0.3^{+0.1}_{-0.1}(m_c)^{+0.7}_{-0.3}(a_i)$	$56.8^{+43.2}_{-56.8}$	$3.9^{+0.7}_{-0.0}(m_c)^{+1.3}_{-1.6}(a_i)$	$78.5^{+7.4}_{-13.9}$
$\Delta S = 0$	$\theta_3 = 38°$		$\theta_K = 50°$	
Decay modes	BRs (10^{-7})	LPFs (%)	BRs (10^{-7})	LPFs (%)
$B_c \to b_1(1235)^+ f_1(1285)$	$2.8^{+4.1}_{-0.5}(m_c)^{+1.8}_{-0.9}(a_i)$	$65.2^{+28.3}_{-16.4}$	$3.0^{+4.4}_{-0.8}(m_c)^{+1.5}_{-0.9}(a_i)$	$68.7^{+21.7}_{-14.6}$
$B_c \to b_1(1235)^+ f_1(1420)$	$1.4^{+0.2}_{-0.1}(m_c)^{+0.7}_{-0.9}(a_i)$	100.0 ± 0.0	$1.2^{+0.4}_{-0.4}(m_c)^{+1.1}_{-0.8}(a_i)$	$100.0^{+0.0}_{-0.8}$

TABLE VI: Same as Table I but for $B_c \to (a_1^+, b_1^+)(h_1(1170), h_1(1380))$ decays.

$\Delta S = 0$	$\theta_1 = 10^\circ$		$\theta_1 = 45^\circ$	
Decay modes	BRs (10^{-6})	LPFs (%)	BRs (10^{-6})	LPFs (%)
$\mathrm{B_c \to a_1(1260)^+ h_1(1170)}$	$1.3^{+0.2}_{-0.5}(m_c)^{+0.5}_{-0.4}(a_i)$	$86.3^{+2.0}_{-9.8}$	$0.7^{+0.2}_{-0.4}(m_c)^{+0.3}_{-0.2}(a_i)$	$73.1^{+7.4}_{-28.8}$
$\mathrm{B_c \to a_1(1260)^+ h_1(1380)} \times 10$	$1.1^{+0.7}_{-0.0}(m_c)^{+1.3}_{-0.5}(a_i)$	$68.8^{+23.2}_{-11.5}$	$6.8^{+0.2}_{-1.1}(m_c)^{+2.3}_{-2.4}(a_i)$	$100.0^{+0.0}_{-1.2}$
$\Delta S = 0$	$\theta_1 = 10^\circ$		$\theta_1 = 45^\circ$	
Decay modes	BRs (10^{-5})	LPFs (%)	BRs (10^{-5})	LPFs (%)
$\mathrm{B_c \to b_1(1235)^+ h_1(1170)}$	$8.1^{+3.6}_{-2.8}(m_c)^{+3.9}_{-3.4}(a_i)$	$96.4^{+1.0}_{-1.6}$	$10.3^{+4.0}_{-3.3}(m_c)^{+4.7}_{-3.8}(a_i)$	$96.4^{+0.9}_{-1.4}$
$\mathrm{B_c \to b_1(1235)^+ h_1(1380)}$	$2.5^{+0.5}_{-0.7}(m_c)^{+1.4}_{-1.2}(a_i)$	$100.0^{+0.0}_{-0.8}$	$0.3^{+0.2}_{-0.1}(m_c)^{+0.5}_{-0.2}(a_i)$	100.0 ± 0.0

for $\theta_K = -45^\circ$, which indicate that one could determine the size and sign of the mixing angle θ_K after enough B_c events become available at the LHC experiments and then improve the precision of the theoretical predictions. In terms of polarization, the longitudinal contributions play the dominated role for both $\theta_K = 45^\circ$ and $\theta_K = -45^\circ$ in $B_c \to \overline{K_1} K^{*+}$ modes. In the $B_c \to \overline{K^*}^0 (K_1(1270)^+, K_1(1400)^+)$ decays, the transverse components govern the former channel for $\theta_K = -45^\circ$ while dominate the latter one for $\theta_K = 45^\circ$. These results will be tested by the relevant measurements in the future.

- Form the numerical results for $B_c \to K_1^+(\rho, \omega)$, the $\Delta S = 1$ processes, as displayed in the

TABLE VII: Same as Table I but for $B_c \to (K_1(1270), K_1(1400))(\rho, K^*, \omega, \phi)$ decays.

$\Delta S = 0$	$\theta_K = 45^\circ$		$\theta_K = -45^\circ$	
Decay modes	BRs (10^{-6})	LPFs (%)	BRs (10^{-6})	LPFs (%)
$\mathrm{B_c \to \overline{K}^{*0} K_1(1270)^+}$	$3.8^{+0.8}_{-0.8}(m_c)^{+3.1}_{-2.7}(a_i)$	$96.8^{+2.5}_{-6.1}$	$2.3^{+0.5}_{-0.4}(m_c)^{+2.9}_{-1.3}(a_i)$	$42.3^{+37.8}_{-30.2}$
$\mathrm{B_c \to \overline{K}^{*0} K_1(1400)^+}$	$2.2^{+0.5}_{-0.4}(m_c)^{+3.0}_{-1.2}(a_i)$	$42.7^{+37.9}_{-29.4}$	$3.8^{+0.8}_{-0.8}(m_c)^{+2.9}_{-2.8}(a_i)$	$96.9^{+2.3}_{-6.1}$
$\mathrm{B_c \to \overline{K_1}(1270)^0 K^{*+}}$	$9.7^{+2.2}_{-2.5}(m_c)^{+5.3}_{-5.1}(a_i)$	$97.5^{+2.6}_{-5.6}$	$5.6^{+2.4}_{-2.1}(m_c)^{+4.3}_{-3.3}(a_i)$	$81.1^{+10.4}_{-17.8}$
$\mathrm{B_c \to \overline{K_1}(1400)^0 K^{*+}}$	$5.8^{+2.2}_{-1.7}(m_c)^{+4.6}_{-3.1}(a_i)$	$82.4^{+9.3}_{-13.8}$	$9.6^{+2.2}_{-2.5}(m_c)^{+5.2}_{-5.1}(a_i)$	$97.6^{+2.4}_{-5.7}$
$\Delta S = 1$	$\theta_K = 45^\circ$		$\theta_K = -45^\circ$	
Decay modes	BRs (10^{-7})	LPFs (%)	BRs (10^{-7})	LPFs (%)
$\mathrm{B_c \to K_1(1270)^0 \rho^+}$	$3.1^{+1.4}_{-1.1}(m_c)^{+2.6}_{-1.7}(a_i)$	$89.5^{+5.9}_{-9.3}$	$4.0^{+1.0}_{-1.2}(m_c)^{+2.2}_{-2.1}(a_i)$	$99.1^{+0.8}_{-3.6}$
$\mathrm{B_c \to K_1(1400)^0 \rho^+}$	$4.0^{+0.9}_{-1.2}(m_c)^{+2.1}_{-2.2}(a_i)$	$99.1^{+0.8}_{-3.4}$	$3.0^{+1.4}_{-1.0}(m_c)^{+2.8}_{-1.5}(a_i)$	$89.7^{+5.6}_{-9.3}$
$\mathrm{B_c \to K_1(1270)^+ \rho^0}$	$1.5^{+0.7}_{-0.5}(m_c)^{+1.4}_{-0.7}(a_i)$	$89.5^{+5.9}_{-9.3}$	$2.0^{+0.5}_{-0.6}(m_c)^{+1.1}_{-1.0}(a_i)$	$99.1^{+0.8}_{-3.6}$
$\mathrm{B_c \to K_1(1400)^+ \rho^0}$	$2.0^{+0.5}_{-0.6}(m_c)^{+1.1}_{-1.0}(a_i)$	$99.1^{+0.8}_{-3.4}$	$1.5^{+0.7}_{-0.5}(m_c)^{+1.4}_{-0.8}(a_i)$	$89.7^{+5.6}_{-9.3}$
$\mathrm{B_c \to K_1(1270)^+ \omega}$	$1.4^{+0.7}_{-0.5}(m_c)^{+1.2}_{-0.7}(a_i)$	$89.8^{+5.4}_{-8.7}$	$1.7^{+0.5}_{-0.5}(m_c)^{+0.9}_{-0.8}(a_i)$	$99.1^{+0.8}_{-3.9}$
$\mathrm{B_c \to K_1(1400)^+ \omega}$	$1.7^{+0.5}_{-0.5}(m_c)^{+0.9}_{-0.9}(a_i)$	$99.1^{+0.8}_{-3.8}$	$1.4^{+0.6}_{-0.5}(m_c)^{+1.1}_{-0.7}(a_i)$	$89.9^{+5.5}_{-8.8}$
$\mathrm{B_c \to K_1(1270)^+ \phi}$	$1.9^{+0.2}_{-0.3}(m_c)^{+1.0}_{-1.4}(a_i)$	$95.2^{+2.7}_{-10.9}$	$1.5^{+0.3}_{-0.4}(m_c)^{+1.2}_{-0.8}(a_i)$	$29.9^{+30.8}_{-27.3}$
$\mathrm{B_c \to K_1(1400)^+ \phi}$	$1.4^{+0.4}_{-0.3}(m_c)^{+1.3}_{-0.6}(a_i)$	$30.3^{+31.0}_{-27.6}$	$1.9^{+0.1}_{-0.3}(m_c)^{+1.0}_{-1.4}(a_i)$	$95.2^{+2.9}_{-10.8}$

Table VII, one can straightforwardly observe that

$$\begin{aligned} Br(B_c \to K_1(1270)^+\omega) &\sim Br(B_c \to K_1(1270)^+\rho^0) \\ &= \frac{1}{2} Br(B_c \to K_1(1270)^0\rho^+) \ ; \end{aligned} \tag{123}$$

$$\begin{aligned} Br(B_c \to K_1(1400)^+\omega) &\sim Br(B_c \to K_1(1400)^+\rho^0) \\ &= \frac{1}{2} Br(B_c \to K_1(1400)^0\rho^+) \ ; \end{aligned} \tag{124}$$

$$\begin{aligned} f_L(B_c \to K_1(1270)^+\omega) &\sim f_L(B_c \to K_1(1270)^+\rho^0) \\ &= f_L(B_c \to K_1(1270)^0\rho^+) \ ; \end{aligned} \tag{125}$$

$$\begin{aligned} f_L(B_c \to K_1(1400)^+\omega) &\sim f_L(B_c \to K_1(1400)^+\rho^0) \\ &= f_L(B_c \to K_1(1400)^0\rho^+) \ . \end{aligned} \tag{126}$$

within errors for both $\theta_K = 45^\circ$ and $\theta_K = -45^\circ$, where the longitudinal components contribute to these considered decays dominantly. The pattern of these decays shown in Eqs. (123-126) can be understood as follows: only the same component $u\bar{u}$ in both of ρ^0 and ω mesons contributes to these physical observables, where the differences mainly arise from the different decay constants. Furthermore, by comparison with $B_c \to \overline{K^*}^0 K_1^+$ and $B_c \to \overline{K_1} K^{*+}$ decays, one can find that the pQCD predictions of $B_c \to K_1^+(\rho, \omega)$ show the weak dependance on the value of the mixing angle θ_K, which will also be tested by the LHC measurements.

- For $B_c \to K_1^+\phi$ decays, it is interesting to note that the decay rates, as listed in Table VII, are close to each other within the theoretical uncertainties, however, the LPFs

TABLE VIII: Same as Table I but for $B_c \to (K_1(1270), K_1(1400))(a_1, b_1, K_1(1270), K_1(1400))$ decays.

$\Delta S = 0$	$\theta_K = 45^\circ$		$\theta_K = -45^\circ$	
Decay modes	BRs (10^{-5})	LPFs (%)	BRs (10^{-5})	LPFs (%)
$\mathrm{B_c \to \overline{K_1}(1270)^0 K_1(1270)^+}$	$1.2^{+0.2}_{-0.1}(m_c)^{+1.8}_{-0.9}(a_i)$	$99.7^{+0.1}_{-1.0}$	$2.9^{+1.2}_{-1.0}(m_c)^{+4.4}_{-2.3}(a_i)$	$71.9^{+16.2}_{-24.6}$
$\mathrm{B_c \to \overline{K_1}(1270)^0 K_1(1400)^+}$	$3.7^{+1.3}_{-1.1}(m_c)^{+3.1}_{-2.2}(a_i)$	$96.2^{+3.5}_{-8.4}$	$1.9^{+0.5}_{-0.5}(m_c)^{+2.2}_{-1.4}(a_i)$	$94.8^{+3.4}_{-10.3}$
$\mathrm{B_c \to \overline{K_1}(1400)^0 K_1(1270)^+}$	$1.9^{+0.5}_{-0.5}(m_c)^{+2.2}_{-1.4}(a_i)$	$94.6^{+3.6}_{-10.7}$	$3.7^{+1.3}_{-1.1}(m_c)^{+3.2}_{-2.1}(a_i)$	$96.1^{+3.6}_{-8.6}$
$\mathrm{B_c \to \overline{K_1}(1400)^0 K_1(1400)^+}$	$2.8^{+1.2}_{-1.0}(m_c)^{+4.3}_{-2.3}(a_i)$	$72.7^{+15.8}_{-24.3}$	$1.1^{+0.2}_{-0.0}(m_c)^{+1.9}_{-0.9}(a_i)$	$99.7^{+0.0}_{-1.0}$
$\Delta S = 1$	$\theta_K = 45^\circ$		$\theta_K = -45^\circ$	
Decay modes	BRs (10^{-7})	LPFs (%)	BRs (10^{-7})	LPFs (%)
$\mathrm{B_c \to K_1(1270)^0 a_1(1260)^+}$	$4.6^{+1.3}_{-1.0}(m_c)^{+4.7}_{-2.4}(a_i)$	$79.2^{+12.4}_{-16.3}$	$8.3^{+1.3}_{-1.8}(m_c)^{+3.6}_{-3.9}(a_i)$	$99.3^{+0.8}_{-5.5}$
$\mathrm{B_c \to K_1(1400)^0 a_1(1260)^+}$	$8.0^{+1.3}_{-1.7}(m_c)^{+3.5}_{-3.7}(a_i)$	$100.0^{+0.0}_{-3.8}$	$4.5^{+1.2}_{-1.1}(m_c)^{+4.4}_{-2.5}(a_i)$	$81.3^{+12.5}_{-16.6}$
$\mathrm{B_c \to K_1(1270)^+ a_1(1260)^0}$	$2.3^{+0.6}_{-0.5}(m_c)^{+2.4}_{-1.3}(a_i)$	$79.2^{+12.4}_{-16.3}$	$4.2^{+0.6}_{-1.0}(m_c)^{+1.8}_{-2.0}(a_i)$	$99.3^{+0.8}_{-5.5}$
$\mathrm{B_c \to K_1(1400)^+ a_1(1260)^0}$	$4.0^{+0.7}_{-0.9}(m_c)^{+1.8}_{-1.9}(a_i)$	$100.0^{+0.0}_{-3.8}$	$2.2^{+0.6}_{-0.5}(m_c)^{+2.3}_{-1.1}(a_i)$	$81.3^{+12.5}_{-16.6}$
$\Delta S = 1$	$\theta_K = 45^\circ$		$\theta_K = -45^\circ$	
Decay modes	BRs (10^{-6})	LPFs (%)	BRs (10^{-6})	LPFs (%)
$\mathrm{B_c \to K_1(1270)^0 b_1(1235)^+}$	$1.6^{+0.8}_{-0.5}(m_c)^{+1.3}_{-0.9}(a_i)$	$91.3^{+5.0}_{-5.1}$	$1.4^{+0.4}_{-0.2}(m_c)^{+0.8}_{-0.7}(a_i)$	$100.0^{+0.0}_{-0.3}$
$\mathrm{B_c \to K_1(1400)^0 b_1(1235)^+}$	$1.3^{+0.4}_{-0.2}(m_c)^{+0.9}_{-0.5}(a_i)$	100.0 ± 0.0	$1.5^{+0.8}_{-0.5}(m_c)^{+1.3}_{-0.9}(a_i)$	$93.6^{+5.0}_{-5.1}$
$\mathrm{B_c \to K_1(1270)^+ b_1(1235)^0}$	$0.8^{+0.4}_{-0.3}(m_c)^{+0.6}_{-0.5}(a_i)$	$91.4^{+4.9}_{-5.1}$	$0.7^{+0.2}_{-0.1}(m_c)^{+0.4}_{-0.4}(a_i)$	$100.0^{+0.0}_{-0.3}$
$\mathrm{B_c \to K_1(1400)^+ b_1(1235)^0}$	$0.7^{+0.2}_{-0.2}(m_c)^{+0.4}_{-0.4}(a_i)$	100.0 ± 0.0	$0.8^{+0.3}_{-0.3}(m_c)^{+0.6}_{-0.5}(a_i)$	$93.6^{+5.1}_{-4.9}$

show us the dramatically different features: the former is dominated by the longitudinal components($\sim$ 95%) while the latter governed by the transverse ones($\sim$ 30%) when $\theta_K = 45^\circ$. The main reason is that the interferences induced by $B_c \to K_{1A}^+\phi$ and $B_c \to K_{1B}^+\phi$ are constructive(destructive) to $B_c \to K_1(1400)^+\phi(B_c \to K_1(1270)^+\phi)$ in the two transverse polarizations, meanwhile, these interferences in the longitudinal polarization contribute to these considered two decays oppositely. When $\theta_K = -45^\circ$, the situation is quite the contrary. The decay mechanism and helicity structure for $B_c \to K_1^+\phi$ decays will be tested by the LHCb and Super-B experiments.

- For the $\Delta S = 0$ processes, $B_c \to \overline{K_1}K_1^+$ modes, as presented in Table VIII, it is of interest to notice that the BRs for all these four considered decays are in the order of 10^{-5}, which are within the reach of B_c experiments at LHC greatly as discussed in Ref. [4]. These numerical results also present the strong dependance on the mixing angle θ_K, which will also be tested by the relevant experiments in the near future. The longitudinal polarization fractions are around 95% $\sim$ 100% within theoretical errors except for $B_c \to \overline{K_1}(1400)^0 K_1(1400)^+$ ($\sim$ 73%) at $\theta_K = 45^\circ$ or $B_c \to \overline{K_1}(1270)^0 K_1(1270)^+$ ($\sim$ 72%) at $\theta_K = -45^\circ$ and paly the dominant role.

- As mentioned in the text above, although the suppressed CKM factor $V_{us} \sim 0.22$ is involved in the decay amplitudes(see Eqs. (95,97,96,98)) for the $\Delta S = 1$ $B_c \to K_1(a_1, b_1)$ decays, the pQCD predictions of the BRs for $B_c \to K_1 b_1$ are in the order of 10^{-6} and larger than that for $B_c \to K_1 a_1$ because the $^1P_1$ meson behaves differently even contrarily to the $^3P_1$ meson, whose behavior is close to that of the vector meson. For the polarization fractions, all of these eight channels are governed by the longitudinal contributions evidently. From the numerical results as given in Table VIII, one can also find that the pQCD predictions of $B_c \to K_1 a_1(B_c \to K_1 b_1)$ are much(less) sensitive to the mixing angle θ_K.

- For the $\Delta S = 1$ $B_c \to K_1^+(f_1(1285), f_1(1420))$ decays, from the pQCD predictions presented in Table IX, one can see that the contributions to the BRs for these four decays come from the overlap of various parts of $B_c \to K_{1A}^+ f_1, K_{1B}^+ f_1, K_{1A}^+ f_8$, and $K_{1B}^+ f_8$, which have been given in Eqs. (99-102). Combining with four mixing parameters $\cos\theta_K$, $\sin\theta_K$, $\cos\theta_3$ and $\sin\theta_3$, these interferences result in the equivalent BRs for

TABLE IX: Same as Table I but for $B_c \to (K_1(1270)^+, K_1(1400)^+)(f_1(1285), f_1(1420))$ decays with $\theta_3 = 38^\circ$(1st entry) and $\theta_3 = 50^\circ$(2nd entry).

$\Delta S = 1$	$\theta_K = 45^\circ$		$\theta_K = -45^\circ$	
Decay modes	BRs (10^{-7})	LPFs (%)	BRs (10^{-7})	LPFs (%)
$\mathrm{B_c \to K_1(1270)^+ f_1(1285)}$	$1.4^{+0.9}_{-0.4}(m_c)^{+2.0}_{-0.7}(a_i)$	$65.1^{+27.4}_{-19.4}$	$1.6^{+0.1}_{-0.5}(m_c)^{+1.1}_{-1.0}(a_i)$	$96.7^{+2.7}_{-11.6}$
	$1.7^{+1.1}_{-0.4}(m_c)^{+2.3}_{-1.0}(a_i)$	$69.1^{+22.1}_{-19.6}$	$1.5^{+0.3}_{-0.6}(m_c)^{+1.6}_{-1.2}(a_i)$	$92.1^{+2.8}_{-13.0}$
$\mathrm{B_c \to K_1(1400)^+ f_1(1285)}$	$1.5^{+0.2}_{-0.4}(m_c)^{+1.2}_{-0.8}(a_i)$	$96.7^{+2.7}_{-11.5}$	$1.4^{+0.8}_{-0.4}(m_c)^{+1.8}_{-0.8}(a_i)$	$65.5^{+27.2}_{-19.4}$
	$1.5^{+0.3}_{-0.6}(m_c)^{+1.6}_{-1.2}(a_i)$	$92.1^{+4.0}_{-12.8}$	$1.7^{+1.1}_{-0.5}(m_c)^{+2.2}_{-1.0}(a_i)$	$69.5^{+21.9}_{-19.6}$
$\mathrm{B_c \to K_1(1270)^+ f_1(1420)}$	$0.9^{+0.4}_{-0.3}(m_c)^{+0.8}_{-0.9}(a_i)$	$81.6^{+13.5}_{-34.6}$	$4.4^{+0.6}_{-0.4}(m_c)^{+1.5}_{-1.7}(a_i)$	$71.5^{+4.8}_{-8.9}$
	$0.6^{+0.1}_{-0.2}(m_c)^{+0.4}_{-0.6}(a_i)$	$78.5^{+16.9}_{-48.1}$	$4.4^{+0.5}_{-0.3}(m_c)^{+1.2}_{-1.5}(a_i)$	$73.2^{+4.8}_{-9.3}$
$\mathrm{B_c \to K_1(1400)^+ f_1(1420)}$	$4.3^{+0.6}_{-0.4}(m_c)^{+1.6}_{-1.7}(a_i)$	$71.9^{+4.8}_{-9.3}$	$0.9^{+0.4}_{-0.3}(m_c)^{+0.8}_{-0.9}(a_i)$	$81.9^{+13.2}_{-34.4}$
	$4.4^{+0.5}_{-0.3}(m_c)^{+1.1}_{-1.6}(a_i)$	$73.6^{+4.8}_{-8.8}$	$0.6^{+0.1}_{-0.2}(m_c)^{+0.4}_{-0.7}(a_i)$	$78.7^{+16.8}_{-47.3}$

$B_c \to K_1(1270)^+ f_1(1285)$ and $B_c \to K_1(1400)^+ f_1(1285)$ decays, and suppressed one for $B_c \to K_1(1270)^+ f_1(1420)$ while enhanced one for $B_c \to K_1(1400)^+ f_1(1420)$. Moreover, (a) the BRs for $B_c \to K_1^+ f_1(1420)(B_c \to K_1^+ f_1(1285))$ depend strongly(weakly) on θ_K for both $\theta_3 = 38^\circ$ and $\theta_3 = 50^\circ$; (b) the BRs for $B_c \to K_1(1270)^+ f_1$ are more sensitive than that for $B_c \to K_1(1400)^+ f_1$ to θ_3 when $\theta_K = 45^\circ$, while the situation is quite the contrary when $\theta_K = -45^\circ$; (c) the longitudinal contributions play an important role in all these considered channels.

- Based on Eq. (3), apart from an overall sign, the physical states $K_1(1270)$ and $K_1(1400)$ can go one into another with changing the mixing angle θ_K from 45° to -45° and vice versa,

$$\begin{aligned} |K_1(1270)\rangle_{\theta_K=45^\circ} &= |K_1(1400)\rangle_{\theta_K=-45^\circ}, \\ |K_1(1400)\rangle_{\theta_K=45^\circ} &= -|K_1(1270)\rangle_{\theta_K=-45^\circ}. \end{aligned} \tag{127}$$

which further results in the decay amplitudes of $B_c \to K_1(V,A)$ (Here, A is a nonstrange axial-vector meson) as follows:

$$\mathcal{A}(B_c \to K_1(1270)(V,A))_{\theta_K=45^\circ} = \mathcal{A}(B_c \to K_1(1400)(V,A))_{\theta_K=-45^\circ}, \tag{128}$$
$$\mathcal{A}(B_c \to K_1(1400)(V,A))_{\theta_K=45^\circ} = -\mathcal{A}(B_c \to K_1(1270)(V,A))_{\theta_K=-45^\circ}. \tag{129}$$

These two relations, i.e., Eqs. (128) and (129), can be manifested by the analytic formulas for $B_c \to K_1(V,A)$ decays as shown in Eqs. (63-66), (69-72), (77-78) and (95-106). The pQCD predictions for these considered $B_c \to K_1(V,A)$ decays as listed in the second and third columns of Tables VII, VIII, IX and X also display the phenomenologies induced by the same pattern.

- For $B_c \to \overline{K_1} K_1^+$ decays, however, it is not the case as shown in Eqs. (128) and (129). According to the relation shown in Eq. (127), there are some simple relations between the decay amplitudes as given in Eqs. (91-94) for $B_c \to \overline{K_1} K_1^+$ decays :

$$\mathcal{A}(B_c \to \overline{K_1}(1270)K_1(1270))_{\theta_K=45^\circ} = -\mathcal{A}(B_c \to \overline{K_1}(1400)K_1(1400))_{\theta_K=-45^\circ}, \tag{130}$$
$$\mathcal{A}(B_c \to \overline{K_1}(1400)K_1(1400))_{\theta_K=45^\circ} = -\mathcal{A}(B_c \to \overline{K_1}(1270)K_1(1270))_{\theta_K=-45^\circ}, \tag{131}$$
$$\mathcal{A}(B_c \to \overline{K_1}(1270)K_1(1400))_{\theta_K=45^\circ} = \mathcal{A}(B_c \to \overline{K_1}(1400)K_1(1270))_{\theta_K=-45^\circ}, \tag{132}$$
$$\mathcal{A}(B_c \to \overline{K_1}(1400)K_1(1270))_{\theta_K=45^\circ} = \mathcal{A}(B_c \to \overline{K_1}(1270)K_1(1400))_{\theta_K=-45^\circ}. \tag{133}$$

TABLE X: Same as Table I but for $B_c \to (K_1(1270)^+, K_1(1400)^+)(h_1(1170), h_1(1380))$ decays with $\theta_1 = 10^\circ$(1st entry) and $\theta_1 = 45^\circ$(2nd entry).

$\Delta S = 1$	$\theta_K = 45^\circ$		$\theta_K = -45^\circ$	
Decay modes	BRs (10^{-6})	LPFs (%)	BRs (10^{-6})	LPFs (%)
$\mathrm{B_c \to K_1(1270)^+ h_1(1170)}$	$1.4^{+0.6}_{-0.6}(m_c)^{+1.3}_{-0.8}(a_i)$	$94.5^{+2.3}_{-3.9}$	$1.6^{+0.7}_{-0.5}(m_c)^{+1.0}_{-1.0}(a_i)$	$98.5^{+0.6}_{-0.9}$
	$0.6^{+0.3}_{-0.3}(m_c)^{+0.3}_{-0.4}(a_i)$	$87.9^{+6.5}_{-14.6}$	$0.2^{+0.2}_{-0.0}(m_c)^{+0.3}_{-0.0}(a_i)$	$92.9^{+7.5}_{-15.1}$
$\mathrm{B_c \to K_1(1400)^+ h_1(1170)}$	$1.6^{+0.7}_{-0.5}(m_c)^{+1.0}_{-1.1}(a_i)$	$98.5^{+0.6}_{-0.9}$	$1.4^{+0.6}_{-0.6}(m_c)^{+1.2}_{-0.9}(a_i)$	$94.6^{+2.3}_{-3.9}$
	$0.2^{+0.2}_{-0.0}(m_c)^{+0.3}_{-0.0}(a_i)$	$93.0^{+7.3}_{-14.8}$	$0.5^{+0.4}_{-0.3}(m_c)^{+0.6}_{-0.2}(a_i)$	$88.1^{+6.4}_{-14.4}$
$\mathrm{B_c \to K_1(1270)^+ h_1(1380)}$	$0.9^{+0.3}_{-0.0}(m_c)^{+0.8}_{-0.3}(a_i)$	$98.5^{+0.8}_{-1.4}$	$1.5^{+0.5}_{-0.4}(m_c)^{+0.9}_{-0.7}(a_i)$	$89.6^{+2.9}_{-4.0}$
	$1.8^{+0.5}_{-0.4}(m_c)^{+1.1}_{-0.9}(a_i)$	$98.6^{+0.8}_{-0.7}$	$2.8^{+1.1}_{-0.8}(m_c)^{+1.7}_{-1.3}(a_i)$	$94.3^{+1.7}_{-2.9}$
$\mathrm{B_c \to K_1(1400)^+ h_1(1380)}$	$1.5^{+0.4}_{-0.4}(m_c)^{+0.8}_{-0.7}(a_i)$	$89.8^{+2.8}_{-3.9}$	$0.9^{+0.3}_{-0.1}(m_c)^{+0.8}_{-0.4}(a_i)$	$98.5^{+0.9}_{-1.3}$
	$2.8^{+1.1}_{-0.8}(m_c)^{+1.6}_{-1.3}(a_i)$	$94.4^{+1.7}_{-2.7}$	$1.7^{+0.6}_{-0.3}(m_c)^{+1.4}_{-0.7}(a_i)$	$98.6^{+0.9}_{-0.5}$

Of course, the above four relations, i.e., Eqs. (130-133), can also be extracted from the pQCD predictions of BRs for $B_c \to \overline{K_1} K_1^+$ decays as presented in Table VIII apart from an overall sign.

- At the first sight, it appears that the numerical results for $B_c \to (f_1, h_1)(V, A)$(Here, A is either a $^3P_1$ or $^1P_1$ nonstrange axial-vector meson) decays are determined by the mixing angles θ_3 and θ_1, respectively, however, based on Ref. [19], whose values will be eventually determined from θ_K in K_{1A}-K_{1B} mixing system. Experimentally, it is thus very important to measure the channels precisely involving $K_1(1270)$ and/or $K_1(1400)$ to determine both of sign and size of the mixing angle θ_K and reduce the uncertainties of theoretical predictions greatly.

- The pQCD predictions for the *CP*-averaged branching ratios of considered B_c decays vary in the range of 10^{-5} to 10^{-9}. Since the LHC experiment can measure the B_c decays with a branching ratio at 10^{-6} level [4], our pQCD predictions for the branching ratios of $B_c \to a_1^+\omega$, $b_1\rho$, $\overline{K^*}^0 K_1^+$, $\overline{K_1^0} K^{*+}$, $\rho^+ f_1(1285)$, $a_1^+ b_1^0$, $b_1^+ a_1^0$, $a_1^+ f_1(1285)$, $a_1^+ h_1(1170)$, $b_1^+ h_1$, $\overline{K_1^0} K_1^+$, $b_1^+ K_1^0$ and $K_1^+ h_1$ decays could be tested in the ongoing LHC experiments.

- It is worth stressing that the theoretical predictions in the pQCD approach still have large theoretical errors induced by the still large uncertainties of many input parameters, e.g. Gegenbauer moments a_i. Any progress in reducing the error of input parameters, such as the Gegenbauer moments a_i and the charm quark mass m_c, will help us to improve the precision of the pQCD predictions.

V. SUMMARY

In summary, we studied the sixty two charmless hadronic $B_c \to VA, AA$ decays by employing the pQCD factorization approach based on the k_T factorization theorem systematically. These considered decay channels can only occur via the annihilation type diagrams in the SM and they will provide an important platform for testing the magnitude and decay mechanism of the annihilation contributions and understanding the helicity structure of these considered channels and the content of the axial-vector mesons. Furthermore, these decay modes might also reveal the existence of exotic new physics scenario or nonperturbative QCD effects.

The pQCD predictions for the *CP*-averaged branching ratios and longitudinal polarization fractions are displayed in Tables (I-X). From our perturbative evaluations and phenomenological analysis, we found the following results:

- The pQCD predictions for the branching ratios vary in the range of 10^{-5} to 10^{-9}. There are many charmless $B_c \to VA, AA$ decays with sizable branching ratios: $B_c \to a_1^+\omega$, $b_1\rho$, $\overline{K^*}^0 (K_1(1270)^+, K_1(1400)^+)$, $(\overline{K_1}(1270)^0, \overline{K_1}(1400)^0) K^{*+}$, $\rho^+ f_1(1285)$, $a_1^+ b_1^0$, $b_1^+ a_1^0$, $a_1^+ f_1(1285)$, $a_1^+ h_1(1170)$, $b_1^+(h_1(1170), h_1(1380))$, $(\overline{K_1}(1270)^0, \overline{K_1}(1400)^0)(K_1(1270)^+, K_1(1400)^+)$, $b_1^+(K_1(1260)^0, K_1(1400)^0)$ and $(K_1(1270)^+, K_1(1400)^+)(h_1(1170), h_1(1380))$, which are with a decay rate at 10^{-6} or larger and could be measured at the LHC experiment.

- For $B_c \to VA, AA$ decays, the branching ratios of $\Delta S = 0$ processes are generally much larger than those of $\Delta S = 1$ ones. Such differences are mainly induced by the CKM factors involved: $V_{ud} \sim 1$ for the former decays while $V_{us} \sim 0.22$ for the latter ones.

- In general, since the behavior for ${}^1P_1$ meson is much different from that for ${}^3P_1$ meson, the branching ratios of the pure annihilation $B_c \to A({}^1P_1)(V, A({}^1P_1))$ are larger than that of $B_c \to A({}^3P_1)(V, A({}^3P_1))$, which can be confronted with the LHC and Super-B experiments.

- The longitudinal contributions play a dominant role in the most of these considered pure annihilation $B_c \to VA, AA$ decays, which will be tested by the ongoing LHC and forthcoming Super-B experiments in the near future.

- The pQCD predictions for several decays involving mixtures of ${}^3P_1$ and/or ${}^1P_1$ mesons are rather sensitive to the values of the mixing angles, which will be tested by the relevant experiments in the future.

- Because only tree operators are involved, the CP-violating asymmetries for these considered B_c decays are absent naturally.

- The pQCD predictions still have large theoretical uncertainties, mainly induced by the uncertainties of the Gegenbauer moments a_i in the meson distribution amplitudes. By reducing these uncertainties dramatically, one can improve the precision of the theoretical predictions effectively.

- We here calculated the branching ratios and polarization fractions of the pure annihilation $B_c \to VA, AA$ decays by employing the pQCD approach. We do not consider the possible long-distance contributions, such as the rescattering effects, although they should be present, and they may be large and affect the theoretical predictions. It is beyond the scope of this work.

Acknowledgments

X. Liu would like to thank You-Chang Yang for reading the manuscript. This work is supported by the National Natural Science Foundation of China under Grant No.10975074, and No.10735080, by the Project on Graduate Students' Education and Innovation of Jiangsu Province, under Grant No. CX09B_297Z, and by the Project on Excellent Ph.D Thesis of Nanjing Normal University, under Grant No. 181200000251.

[1] N. Brambilla *et al.*, (Quarkonium Working Group), CERN-2005-005, arXiv:0412158[hep-ph].
[2] X. Liu, Z.J. Xiao, and C.D. Lü, Phys. Rev. D **81**, 014022 (2010).
[3] X. Liu and Z.J. Xiao, Phys. Rev. D **81**, (2010) in press, arXiv:1001.2944[hep-ph].
[4] S. Descotes-Genon, J. He, E. Kou, and P. Robbe, Phys. Rev. D **80**, 114031 (2009).
[5] G. Buchalla, A.J. Buras and M.E. Lautenbacher, Rev. Mod. Phys. **68**, 1125 (1996).
[6] Y.Y. Keum, H.N. Li, and A.I. Sanda, Phys. Lett. B **504**, 6 (2001); Phys. Rev. D **63**, 054008 (2001).
[7] C.D. Lü, K. Ukai, and M.Z. Yang, Phys. Rev. D **63**, 074009 (2001).
[8] H.N. Li, Prog. Part. & Nucl. Phys. **51**, 85 (2003), and reference therein.
[9] C.D. Lü and K. Ukai, Eur. Phys. J. C **28**, 305 (2003).
[10] H.N. Li, and S. Mishima, Phys. Rev. D **71**, 054025 (2005); H.N. Li, Phys. Lett. B **622**, 63 (2005).
[11] X. Liu, H.S. Wang, Z.J. Xiao, L.B. Guo, and C.D. Lü, Phys. Rev. D **73**, 074002 (2006); H.S. Wang, X. Liu, Z.J. Xiao, L.B. Guo, and C.D. Lü, Nucl. Phys. B **738**, 243 (2006); Z.J. Xiao, X.F. Chen, and D.Q. Guo, Eur. Phys. J. C **50**, 363 (2007); Z.J. Xiao, D.Q Guo, and X.F. Chen, Phys. Rev. D

75, 014018 (2007); Z.J. Xiao, X. Liu, and H.S. Wang, Phys. Rev. D **75**, 034017 (2007); Z.J. Xiao, X.F. Chen, and D.Q. Guo, arXiv:0701146[hep-ph].
[12] A. Ali, G. Kramer, Y. Li, C.D. Lü, Y.L. Shen, W. Wang, and Y.M. Wang, Phys. Rev. D **76**, 074018 (2007);
[13] Z.J. Xiao, Z.Q. Zhang, X. Liu, and L.B. Guo, Phys. Rev. D **78**, 114001 (2008).
[14] C.H. Chen and H.N. Li, Phys. Lett. B **561**, 258 (2003); Phys. Rev. D **70**, 054006 (2004).
[15] B.H. Hong and C.D. Lü, Sci. China G **49**, 357 (2006).
[16] A.V. Gritsan, Econf C **070512**, 001 (2007); A.L. Kagan, Phys. Lett. B **601**, 151 (2004).
[17] H.J. Lipkin, Phys. Lett. B **72**, 249 (1977); M. Suzuki, Phys. Rev. D **47**, 1252 (1993); L. Burakovsky and T. Goldman, Phys. Rev. D **56**, R1368 (1997); H.Y. Cheng, Phys. Rev. D **67**, 094007 (2003); H.Y. Cheng and C.K. Chua, Phys. Rev. D **69**, 094007 (2004); H.Y. Cheng, C.K. Chua, and C.W. Hwang, Phys. Rev. D **69**, 074025 (2004);
[18] K.C. Yang, Phys. Rev. D **72**, 034009 (2005); Phys. Rev. D **72**, 059901(E) (2005); C.H. Chen, C.Q. Geng, Y.K. Hsiao, and Z.T. Wei, Phys. Rev. D **72**, 054011 (2005); G. Nardulli and T.N. Pham, Phys. Lett. B **623**, 65 (2005); V. Laporta, G. Nardulli, and T.N. Pham, Phys. Rev. D **74**, 054035 (2006); Phys. Rev. D **76**, 079903(E) (2007).
[19] K.C. Yang, J. High Energy Phys. **0510**, 108 (2005); Nucl. Phys. B **776**, 187 (2007).
[20] H.Y. Cheng and K.C. Yang, Phys. Rev. D **76**, 114020 (2007).
[21] K.C. Yang, Phys. Rev. D **76**, 094002, (2007);H. Hatanaka and K.C. Yang, Phys. Rev. D **77**, 094023 (2008); Phys. Rev. D **78**, 059902(E) (2008); K.C. Yang, Phys. Rev. D **78**, 034018 (2008); H. Hatanaka and K.C. Yang, Phys. Rev. D **78**, 074007 (2008).
[22] W. Wang, R.H. Li, and C.D. Lü, Phys. Rev. D **78**, 074009 (2008).
[23] H.Y. Cheng and K.C. Yang, Phys. Rev. D **78**, 094001 (2008).
[24] R.H. Li, C.D. Lü, and W. Wang, Phys. Rev. D **79**, 034014 (2009).
[25] C. Amsler *et al.*, (Particle Data Group), Phys. Lett. B **667**, 1 (2008).
[26] Heavy Flavor Averaging Group, E. Barberio *et al.,* arXiv:0808.1297[hep-ex]; and online update at http://www.slac.stanford.edu/xorg/hfag.
[27] J.F. Cheng, D.S. Du and C.D. Lü, Eur. Phys. J. C **45**, 711 (2006).
[28] J. Sun, Y. Yang, W. Du and H. Ma, Phys. Rev. D **77**, 114004 (2008); J. Sun, G. Xue, Y. Yang, G. Lu and D. Du, Phys. Rev. D **77**, 074013 (2008); J. Sun, D. Du and Y. Yang, Eur. Phys. J. C **60**, 107 (2009).
[29] P. Ball, V.M. Braun, Y. Koike and K. Tanaka, Nucl. Phys. B **529**, 323 (1998); P. Ball and V.M. Braun, Nucl. Phys. B **543**, 201 (1999).
[30] P. Ball and V.M. Braun, Phys. Rev. D **54**, 2182 (1996); P. Ball and R. Zwicky, J. High Energy Phys. **02** (2006) 034; P. Ball and M. Boglione, Phys. Rev. D **68**, 094006 (2003).
[31] P. Ball and R. Zwicky, J. High Energy Phys. **04** (2006) 046.
[32] P. Ball and R. Zwicky, Phys. Rev. D **71**, 014029 (2005).
[33] P. Ball and G.W. Jones, J. High Energy Phys. **03** (2007) 069.
[34] H.N. Li, Phys. Rev. D **66**, 094010 (2002).
[35] H.N. Li and B. Tseng, Phys. Rev. D **57**, 443 (1998).